

CT Imaging

Acquisition and
Interpretation Techniques
for Transcatheter Aortic Valves



Edwards

Edited by:
Philipp Blanke, MD
Cardiac Radiologist
Center for Heart Valve Innovation
St. Paul's Hospital
Vancouver

Jonathon Leipsic, MD, FSCCT
Cardiac Radiologist
Center for Heart Valve Innovation
St. Paul's Hospital
Vancouver

Erin Fletcher RN, BSN, RCIS
Global Product Training Manager,
Imaging, Procedure, and Patient Initiatives
Edwards Lifesciences, THV – Global

Kyle Bilhorn, MPH, RDCS, FASE
Manager, Clinical Affairs
Core Laboratories and Imaging
Edwards Lifesciences, THV – Global

This reference book is provided as an educational resource to medical personnel by Edwards Lifesciences (the "Author"). The information in this reference book has been compiled from then-currently available literature. Although every effort has been made to faithfully report the information and keep it up to date, the Author cannot be held responsible for the completeness or accuracy. This reference book is not intended to be and should not be construed as medical advice. For any use, the product information guides, inserts, and operation manuals of the drugs and devices should be consulted. Edwards Lifesciences, and their respective affiliates disclaim any liability arising directly or indirectly from the use of drugs, devices, techniques, or procedures described in this reference book.

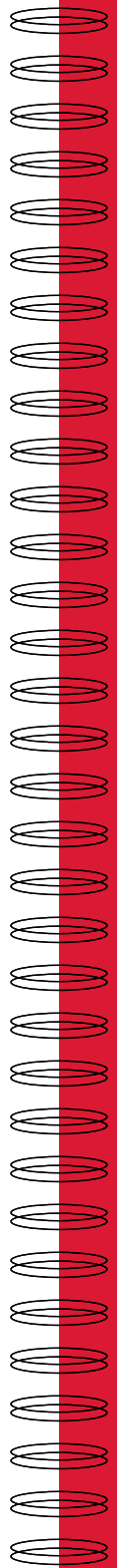
WARNING: Any reference to X-ray exposure, intravenous contrast dosage, and other medication is intended as a reference guideline only. The guidelines in this document do not substitute for the judgment of a health care provider. Each scan requires medical judgment by the health care provider about exposing the patient to ionizing radiation. Use the As Low As Reasonably Achievable (ALARA) radiation dose principle to balance factors such as the patient's condition, size, and age; region to be imaged; and diagnostic task.

NOTE: Algorithms/protocols included in this reference book are for educational reference only. The authors do not endorse or support any one specific algorithm/protocol. It is up to each individual clinician and institution to select the treatment that is most appropriate.

Philipp Blanke, MD is a paid consultant for Edwards Lifesciences

Table of Contents

Acquisition	5
• Acquisition Recommendations for Combined Assessment of the Aortic Root and Aorto-Iliofemoral Vasculature.....	7
Image Reconstruction	17
Annular Plane	23
• Definition and Identification of the Aortic Annulus and the Annular Plane.....	25
• Techniques for Determining the Annular Plane.....	26
Measurements	31
• Annular and Aortic Root Measurements.....	33
• Pre-procedural Assessment for Aortic Valve-in-Valve Procedures.....	46
• Pre-procedural Assessment for Mitral Valve-in-Valve Procedures.....	51
• Bicuspid Aortic Valve.....	54
Access	61
• Transfemoral Access Analysis.....	63
• Subclavian and Axillary Access Analysis.....	70
• Additional Assessment for Transaortic or Transapical Approach	74
• Assessment for Transseptal Access.....	76
Troubleshooting	79
• ECG-Editing.....	90
Bibliography	95



Acquisition Recommendations for Combined Assessment of the Aortic Root and Aorto-Iliofemoral Vasculature

Contrast-enhanced computed tomography (CT) allows for anatomical assessment of the aortic root and the aortoiliac vasculature within a single examination. Data acquisition strategies and scanning protocols may vary based on scanner-system and institutional preferences. The key component of all approaches is an ECG-assisted data acquisition, which covers at least the aortic root, while the remainder of the data acquisition may be performed without ECG assistance. If employed properly, ECG assistance allows for artifact-free depiction of the aortic root.

The sequence of patient preparation and data acquisition and the relevant principles of CT data acquisition will be explained in brief below.

ECG-assisted CT Data Acquisition

ECG-assisted CT data acquisition implies that in parallel to the CT data acquisition, the patient's ECG signal is recorded to do the following:

- Direct the data acquisition itself
- Direct the image reconstruction

For CT systems with limited detector coverage, there are currently three different types of ECG-assisted data acquisition techniques:

- Retrospective ECG-gating
- Prospective ECG-triggering
- High-pitch helical

CT scanners with whole-heart coverage, known as volume CT scanners, commonly use one beat/one slab volume acquisition, often referred to as ECG-gating.

See **TABLE 1** for recommended ECG-assisted acquisition techniques by scanner manufacturer.

Recommendation:

Independent of the scanner system being used, it is recommended that the entire cardiac cycle be imaged maintaining diagnostic image quality throughout. Coverage of the entire cardiac cycle is important for:

- Determining largest annular dimensions

- Determining valve morphology
- Providing redundant image data for artifact mitigation

For scanners with limited detector coverage (64 slice scanners), employment of retrospective ECG-gating is recommended.

Recommended ECG-assisted acquisition techniques stratified by scanner manufacturer:

Scanner	Detector coverage	Recommendation	
GE	GE Revolution (volume scanner)	16 cm	ECG-gated, one-beat, one-slab volume acquisition
	CardioGraphe	14 cm	ECG-gated, one-beat, one-slab volume acquisition
	Other GE scanners	4 cm	Helical/spiral acquisition with retrospective ECG-gating
Philips	iCT 256	8 cm	Helical/spiral acquisition with retrospective ECG-gating, or ECG-gated, one-beat, one-slab volume acquisition
	Other Philips scanners	≤4 cm	Helical/spiral acquisition with retrospective ECG-gating
Siemens	Siemens Dual-Source (SOMATOM Definition, Flash, Force)	5.76 cm (Force) 3.84 cm (Flash/Drive) 1.92 cm (Definition)	Helical/spiral acquisition with retrospective ECG-gating (do not use high-pitch helical acquisition or step-and-shoot mode)
	Single-source Siemens scanners	≤3.84 cm	Helical/spiral acquisition with retrospective ECG-gating
Canon (formerly Toshiba Medical Systems)	Aquilion ONE Vision/Genesis (16 cm) Aquilion Premium (8 cm)	16 cm	ECG-gated, one-beat, one-slab volume acquisition
	Other Toshiba scanners	≤4 cm	Helical/spiral acquisition with retrospective ECG-gating

Table 1

Recommended ECG-gated helical data acquisition without dose modulation

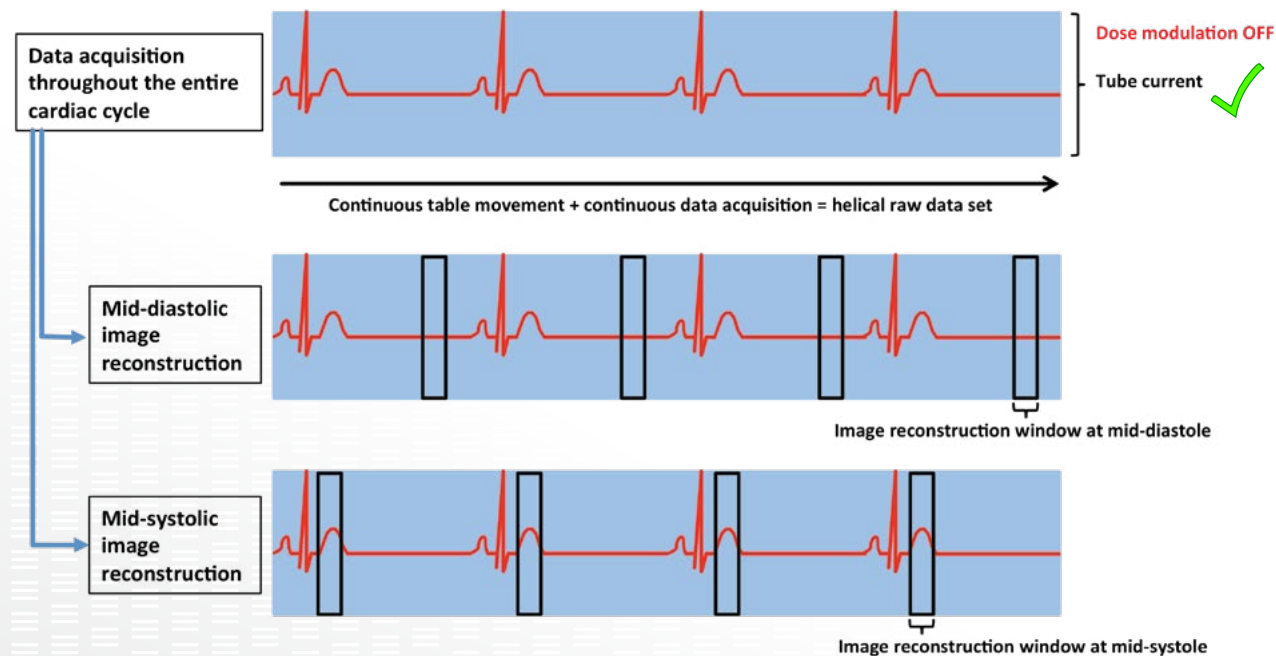


Figure 1. Retrospective ECG-gated helical data acquisition without dose modulation. The tube current (blue bar) is set at its peak during the entire cardiac cycle. The black boxes indicate the time point of image reconstruction within the cardiac cycle.

Retrospective ECG-Gating Is Characterized by:

- Helical/spiral data acquisition due to continuous movement of the patient through the gantry while the scanner gantry rotates.
- Simultaneous recording of the ECG signal.
- The recorded ECG signal allows for retrospective image reconstruction at specific time points of the cardiac cycle (FIGURE 1).
- In general, this technique is available on all scanner platforms capable of cardiac CT scans.
- **Advantage.** Allows for dynamic (cine) imaging/ image reconstruction throughout the entire cardiac cycle (early systole–late diastole).
- **Advantage.** Greater flexibility in unstable heart rates or rhythms, (eg, atrial fibrillation or premature ventricular contractions) ability to use data from different phases (systole or diastole) and to manually edit the reconstruction (please refer to section ECG-Editing in Chapter 6).
- **Disadvantage.** Relatively high radiation dose when full tube current is applied throughout the entire cardiac cycle.

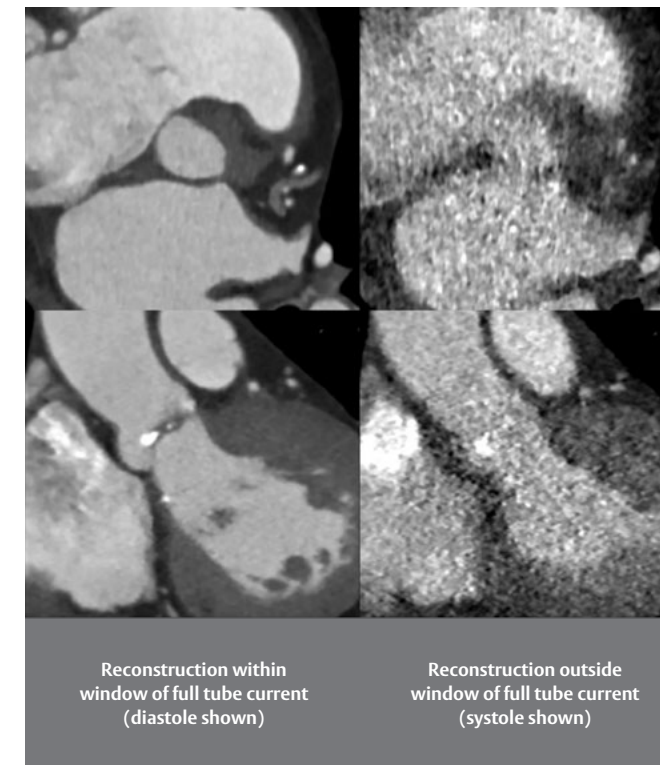


Figure 2. Example of retrospective ECG-gating with dose modulation during systole (not recommended). Images reconstructed during systole outside the window of peak tube current are noisy and uninterpretable.

Recommendation:

1. Acquire contrast-enhanced, ECG-assisted CT data of the aortic root covering the entire cardiac cycle.
2. Use recommended ECG-assisted acquisition technique for scanner system identified in TABLE 1.
 - Ideally, dose modulation should be disabled to allow for data acquisition with peak tube current throughout the entire cardiac cycle; however, if utilized, it is recommended that dose modulation be used only in diastole set to 20% to 30% of peak dose.

- It is not recommended to use dose modulation in systole.

CAVEAT: Most automated coronary CTA protocols with dose modulation reduce tube current during systole.

- ECG-editing should be considered to reduce artifacts due to premature contractions or atrial fibrillation.

See Chapter 6 for additional information on ECG-editing.

Retrospective ECG-gated helical data acquisition with dose modulation—lowered tube current during systole ❌❌

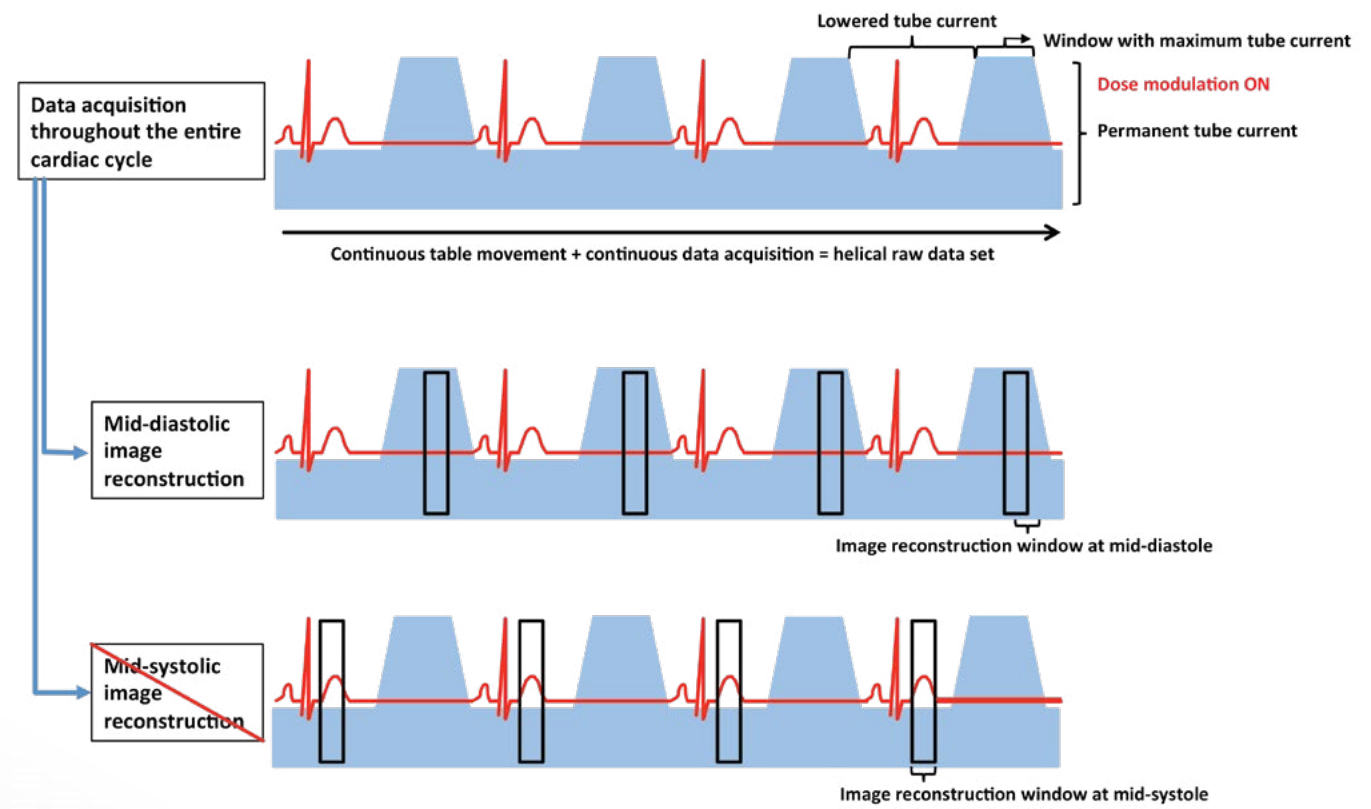


Figure 3. Retrospective ECG-gated helical data acquisition with dose modulation. Peak tube current is limited to mid-diastole (not recommended). Image reconstruction at systole (lower row) will likely result in uninterpretable image quality.

Dose modulation in retrospective ECG-gating

- Dose modulation is modulation of the tube current throughout the cardiac cycle with peak tube current (mAs) during a predefined phase of the cardiac cycle and lowered tube current during the remainder of the cardiac cycle (FIGURES 3 and 4).
- Although image reconstruction is still technically feasible throughout the cardiac cycle, images reconstructed outside the preselected phase will

have increased image noise and may not be interpretable (FIGURE 2).

- For aortic root evaluation, images are usually uninterpretable if tube current is lowered below **one-third** of the peak current.
- Due to the pulsatile and conformational changes of the aortic annulus throughout the cardiac cycle with larger dimensions usually found in systole, **peak tube current is warranted during systole.**

Retrospective ECG-gated helical data acquisition with dose modulation—lowered tube current during diastole ❌

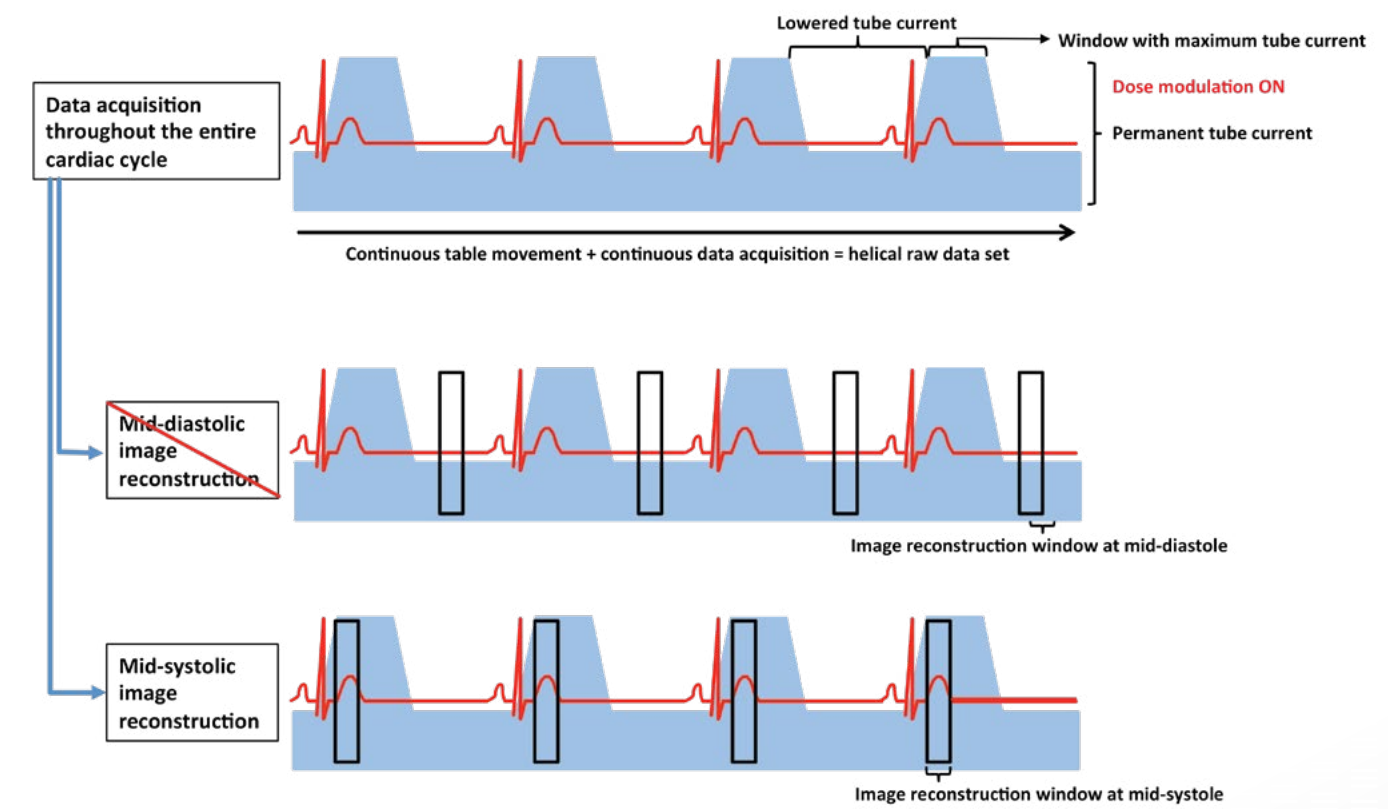
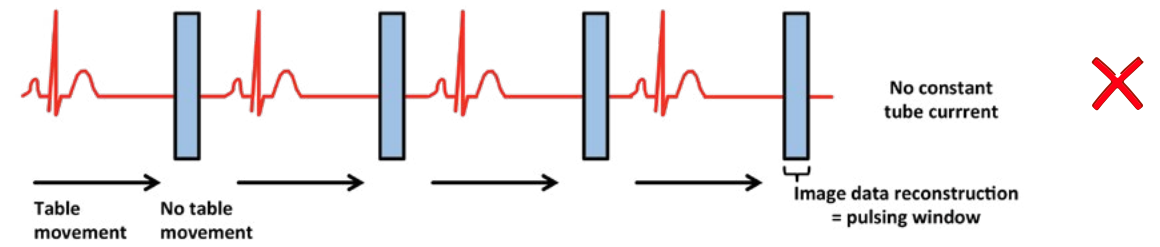


Figure 4. Retrospective ECG-gated helical data acquisition with dose modulation. Peak tube current is limited to systole. Image reconstruction at diastole (middle row) will likely result in uninterpretable image quality.

- **Advantage:** Radiation dose reduction.
- **Disadvantage:** Images reconstructed outside the window of full/peak tube current have increased image noise and may be uninterpretable.

Diastolic image acquisition



Systolic image acquisition

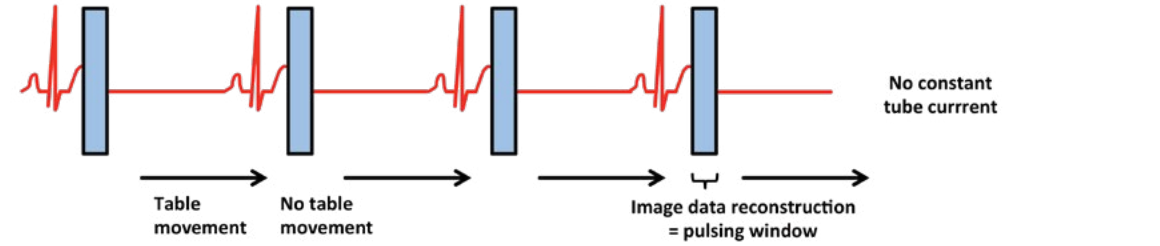


Figure 5. Prospective ECG-triggered sequential data acquisition. Upper row with diastolic data acquisition (not recommended), lower row with systolic data acquisition.

Prospective ECG-Triggering Is Characterized by:

- Data acquisition is prospectively triggered by the ECG signal (FIGURE 5).
- Data acquisition is performed in a slab-wise (sequential axial, nonhelical) fashion while the patient table does not move; the table is moved in between slabs.
- Acquisition windows are usually limited to a specific portion of the cardiac cycle (eg, only mid-diastole) with no radiation exposure or image acquisition occurring outside the acquisition window.
- Limiting the extent of the acquisition window often allows for only a single reconstruction or, if the window is broadened (“padding”), for slight variation in the reconstruction window.
- **Advantage:** Lower radiation dose.
- **Disadvantage:** Allows for only limited coverage of the cardiac cycle and almost no correction in case of increased heart rate variability, misregistration or motion artifact. This approach is susceptible to step-artifact in case of increased heart rate variability. Even broadening the acquisition window will not mitigate step artifacts.

High-Pitch Helical Data Acquisition

- High-pitch helical data acquisition is limited to second- and third-generation dual-source scanners and employs high-pitch factors implying large table feed per gantry rotation.
- Data acquisition can be ECG-triggered to aim for systolic or diastolic data acquisition at the level of the aortic root.
- This technique allows for only a single reconstruction.

- **Advantage:** Low radiation exposure.
- **Disadvantage:** Allows for only a single reconstruction with no potential for correction in the case of artifact. ECG-triggering is typically unreliable with increased heart rate variability, such as in atrial fibrillation.

Recommendation:

- Due to the limited amount of image data acquired and the very limited potential for image salvage in case of artifacts, prospective ECG-gated and high-pitch helical data acquisition are not recommended.
- If prospective ECG-triggering is employed, the acquisition window should be centered in systole.

Volume Scanners

Volume scanners with wide z-axis coverage (eg, 256-slice or 320-slice CT scanners with 16 cm coverage) are capable of covering the entire aortic root with one slab using axial data acquisition and prospective triggering (commonly referred to as ECG-gating). By extending the acquisition window to cover the entire cardiac cycle, this technique may allow for dynamic imaging and may then be considered equivalent to retrospective ECG-gating without dose modulation (FIGURE 6).

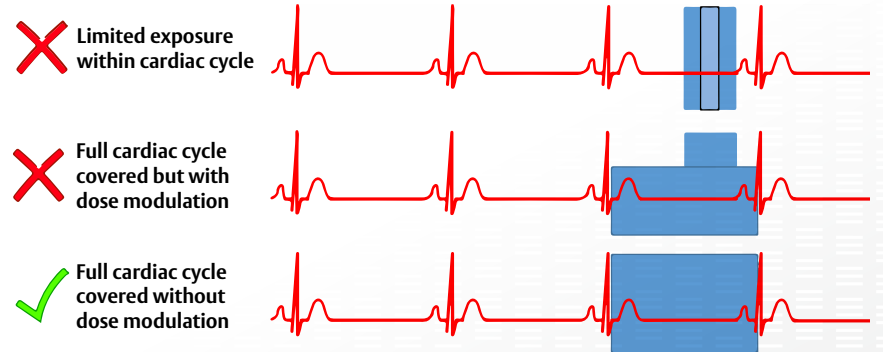


Figure 6. Volume CT with whole-heart coverage: Covers the entire cardiac cycle without dose modulation, using a one-beat, one-slab data acquisition (also referred to as ECG-gating).

CT scan -- Patient preparations

- Positioning of the patient on the scanner table, typically supine, should closely resemble positioning on the cath lab table.
- Placement of ECG electrodes and IV access should follow institutional policies.
- Patient instruction on breath-holding prior to scanning may improve compliance during the scan.

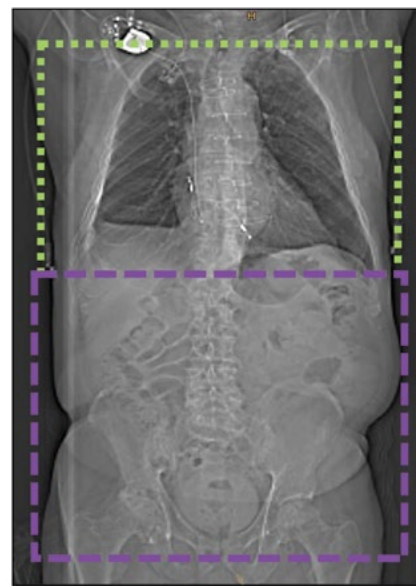
Cardiac ECG-assisted data acquisition



+
Non-gated CTA of the thorax, abdomen, and pelvis

Preferred method

ECG-assisted data acquisition of the thorax



+
Non-gated CTA of the abdomen and pelvis

Figure 7. Scout views highlighting two different imaging strategies: left: ECG-assisted data acquisition limited to the aortic root and heart (green box) followed by non-gated CTA of the thorax, abdomen, and pelvis (purple box); right: ECG-assisted data acquisition of the entire thorax (green box) followed by the non-gated CTA of the abdomen and pelvis (purple box).

CT Scan – Scan Length and Scan Strategy

In general, there are two different approaches on how to combine the ECG-assisted data acquisition of the aortic root structures and the non-ECG-assisted computed tomography angiography (CTA) of the aortoiliofemoral vasculature for evaluation of the transfemoral access route (FIGURE 7):

1.) Preferred

Cardiac ECG-assisted data acquisition of the heart and aortic root (usually beginning 2 cm below the carina) followed by a non-ECG-assisted CTA of the thorax, abdomen, and pelvis. Although this approach results in repeat data acquisition of the aortic root and cardiac structures, the radiation dose intensive ECG-assisted data acquisition is kept to a minimum.

2.) Alternative

ECG-assisted data acquisition of the thorax followed by a non-ECG-assisted CTA of the abdomen and pelvis. The disadvantage of this approach is the higher radiation dose and the relatively long acquisition time required for the entire thorax (may exceed 15 seconds), which increases the risk of breathing artifacts at the level of the cardiac structures.

Recommendation

In General

- All studies should be acquired using smallest available slice thickness (≤ 0.75 mm) based on individual system capabilities.
- The scan coverage for the ECG-gated portion of the scan should cover, at a minimum, the aortic root. The entire heart can be covered if the scan is used to interpret the coronary arteries. Scan coverage should thus be adjusted to institutional requirements and policies. However, the ECG-gated portion should not cover the entire chest in order to limit radiation dose.
- The scan coverage for the non-ECG-assisted CTA should include the aortic arch and extend to shortly above the lesser trochanter.
- If your institution has the capabilities of alternate access strategies via the subclavian arteries, the scan range should be extended to cover the entire upper thoracic inlet.
- The data acquisition of the non-ECG-assisted CTA should be performed in cranial to caudal direction.
- Tube voltage, tube current, and pitch should be adapted to institutional CTA protocols.

IV Contrast Administration

- The total dose of contrast administered varies with scanner, imaging protocol, and body habitus, typically ranging from 60 to 100 mL/s.
- Image acquisition timing can be performed using either a timing bolus (test bolus) or bolus tracking. Bolus tracking with a region of interest (eg, in the ascending aorta) is less cumbersome and usually sufficient for imaging of the aortic root.
- Specific contrast protocols should follow institutional policies. A minimum injection rate of approximately 3 to 4 mL/s is usually required to allow for sufficient contrast attenuation of the aortic root.

ECG-Editing With Retrospective ECG-Gating

- The in-part redundant image data that is acquired using helical/spiral data acquisition with retrospective ECG-gating allows for manual editing of the ECG signal with adjustment or deletion of certain trigger points (eg, an entire heart beat may be deleted, in case of a premature contraction).

- This technique should be employed in cases of misalignment artifacts due to premature contractions or atrial fibrillation.
- ECG-editing has to be performed at the scanner console using the raw data.

CAVEAT: Raw data is typically stored for only a limited time.

See Chapter 6 for additional information on ECG-editing.

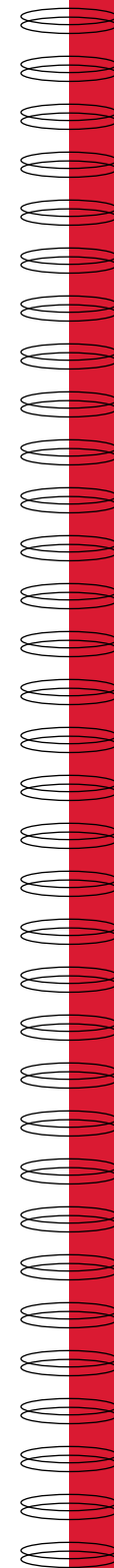


Image Reconstruction

CT images are reconstructed on the scanner console from so-called raw data, which is the data acquired during the scan. One reconstructed image requires at least 180 degrees (half rotation) of image data. This implies that one reconstructed image is always subject to temporal averaging, with usually 65 msec to 175 msec image data contributing to one image (depending on rotation time and single- versus dual-source technology).

Relative Versus Absolute Reconstruction

Retrospective ECG-gating synchronizes the CT image data acquired over the course of multiple heartbeats by means of the recorded ECG signal. Historically, CT images have been reconstructed using a **relative** approach by assigning the position of the reconstruction window within the R-to-R interval in a percentage approach (FIGURE 8).

Alternatively, on platforms manufactured by General Electric, Siemens, and Canon (formerly Toshiba), CT images can be reconstructed using **absolute** reconstruction, which assigns the position of the reconstruction window within the R-to-R interval as a fixed (absolute) distance to the R-peak in milliseconds (msec).

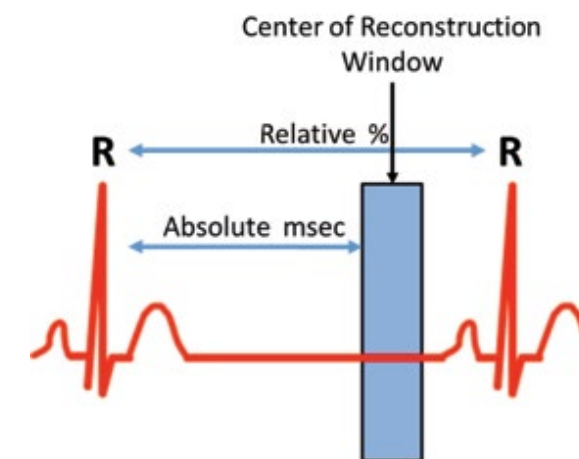


Figure 8. Relative versus absolute reconstruction.

Multiphasic reconstructions

Multiphasic (or cine, functional, 4D) data sets consist of multiple reconstruction windows in defined increments, covering parts of or the entire cardiac cycle (**FIGURE 9**). Routinely employed increments are:

- 5% or 10%, when using relative reconstruction
- 50 msec, when using absolute reconstruction

Practical differences in relative versus absolute reconstructions

- CT scanners with limited detector coverage (eg, 64-slice CT): Absolute reconstruction results in superior image quality, compared to relative reconstruction in the setting of increased heart rate variability as seen with atrial fibrillation or premature contractions.
- Volume CT scanners: There is no practical difference in image quality when comparing relative and absolute image reconstruction, independent of heart rhythm or heart rate.
- In the setting of regular sinus rhythm, both reconstruction techniques result in similar image quality and image content.

- Relative reconstruction at a defined increment always results in the same number of reconstruction phases (eg, 10 phases at 10% increments when reconstructing 0%-90%), independent of the heart rate. If the heart rate is faster, R-to-R intervals are shorter, with subsequent closer stacking of the reconstruction windows. If the heart rate is lower, R-to-R intervals are longer, with subsequent looser stacking of the reconstruction windows.
- Absolute reconstruction at a defined increment results in fewer reconstruction phases if heart rate is higher, given the shortening of the R-to-R intervals (eg, 21 reconstruction phases covering 0-1,000 msec at 50 msec increments for 60 bpm, 16 reconstruction phases covering 0-750 msec at 50 msec increments for 80 bpm); however, this has no relevance for image interpretation when planning for a transcatheter heart-valve procedure.

End-systolic image reconstruction

- End-systole is the most stable phase within the cardiac cycle, in regard to variation with changing heart rate variability and heart rate.
- In particular, in patients with atrial fibrillation or frequent premature contractions, the best image quality can be found at end-systole.
- In these scenarios, commonly encountered stair-step artifacts are more pronounced in diastole, given the impact of heart rate variability on LV filling state.

ECG-Assisted Image Data of the Aortic Root/Heart

- A small reconstruction field of view should be used to allow for maximum spatial resolution.
- The thinnest possible slice thickness should be employed (eg, 0.6 or 0.75 mm).
- If retrospective ECG-gating is employed, image reconstructions should cover the entire cardiac cycle (multiphasic data set).

Reconstruction

- Relative reconstruction: 0%-90% R-to-R intervals at 10% increments
- Absolute reconstruction: 50 msec increments
- Traditional filtered back projection or iterative reconstruction may be used.

Non-ECG-Assisted Image Data of the Thorax, Abdomen, and Pelvis

- The slice thickness should be no thicker than 1.5 mm.
- Traditional filtered back projection or iterative reconstruction may be used.

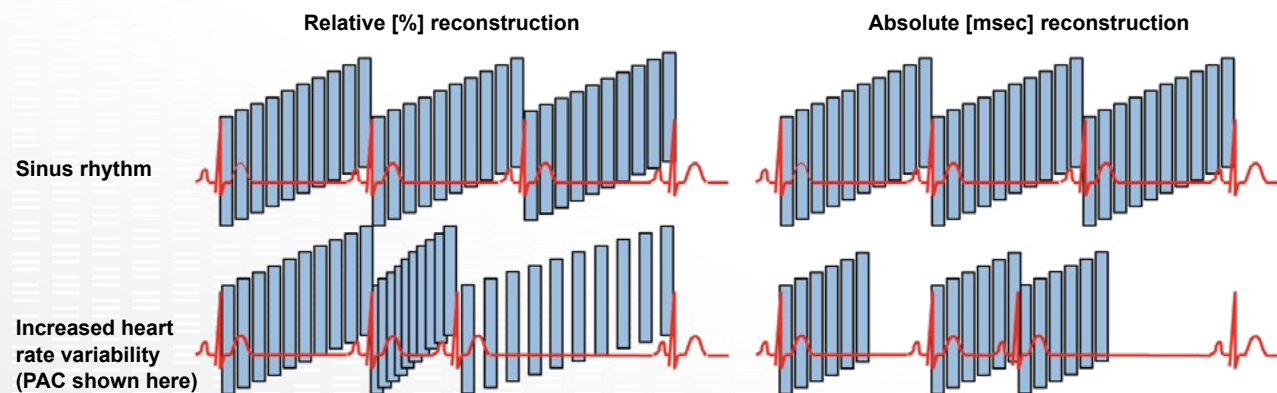
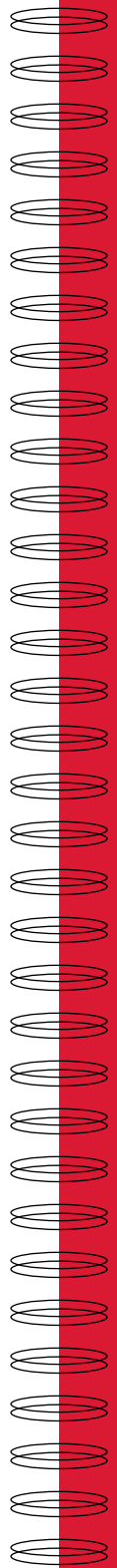


Figure 9. Multiphasic reconstructions using relative (%) and absolute (msec) reconstruction techniques in sinus rhythm and increased heart rate.



Definition and Identification of the Aortic Annulus and the Annular Plane

The aortic annulus is not a discrete structure; rather, it is a virtual ring formed by the three lowest attachment points of the aortic valve cusps, or hinge points (**FIGURE 10**). Accurately identifying the aortic annular plane is fundamental to proper transcatheter heart valve prosthesis size selection.

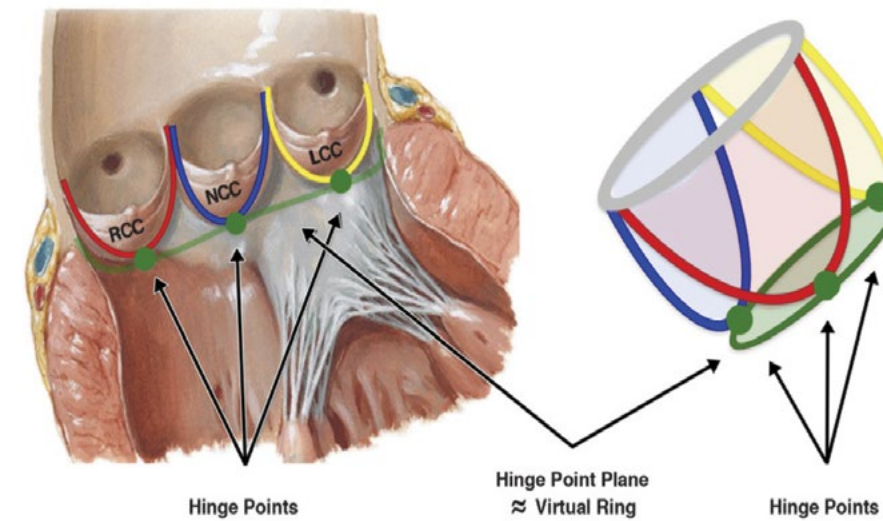


Figure 10. Aortic root anatomy and definition of the annular plane. (Image source: Kasel et al. JACC: Cardiovascular Imaging. February 2013.)

Nomenclature of Viewing Planes

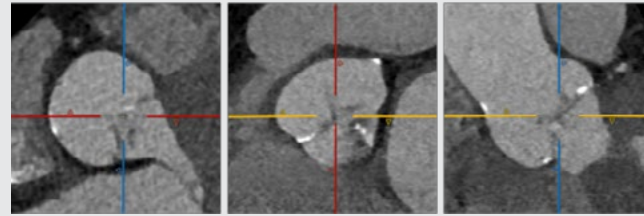
CT images are commonly viewed using multiplanar reformats (MPR). Post-processing platforms provide an axial (transverse), coronal, and sagittal view at the very beginning of processing. Exact orientation of one imaging view is indicated by the crosshairs in the

two remaining views. Manipulating the orientation of the crosshairs results in a oblique or double-oblique orientation of the dependent views, such as a sagittal double-oblique view.

Techniques for Determining the Annular Plane

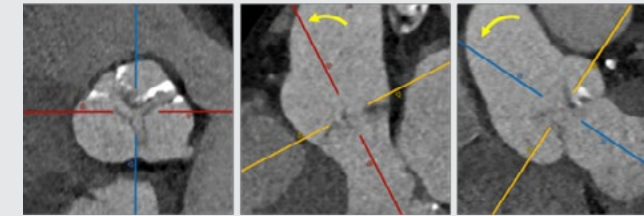
There are multiple ways of identifying the correct annular plane using MPRs. Independent of the approach, the final double-oblique transverse view should transect the hinge points of the three aortic valve cusps.

A systematic, stepwise approach has been published by the Society of Cardiovascular Computed Tomography.



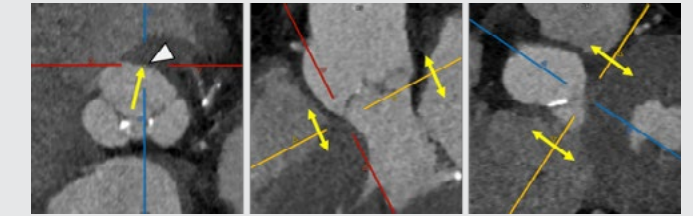
Step 1

Start out with multiplanar images in default axial, sagittal, and coronal orientation; center crosshairs onto the aortic valve.



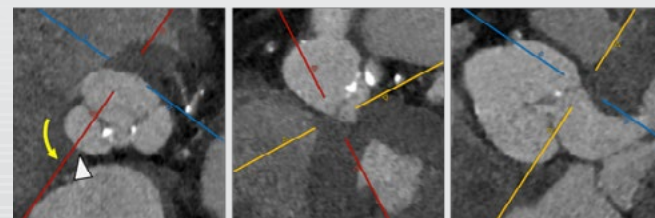
Step 2

Align the crosshairs in the sagittal and coronal views with the long axis of the aortic root; the resulting double-oblique transverse view will depict the aortic valve en face.



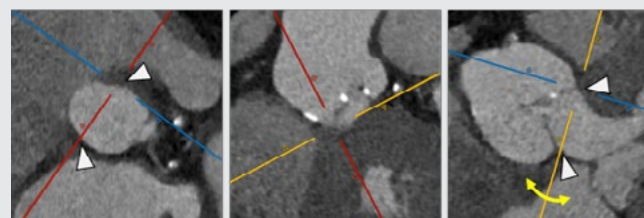
Step 3

Move the double-oblique transverse plane up and down to identify the lowest insertion point of the right coronary cusp, which is usually located at about 1 o'clock. Position the center of the crosshairs exactly at the most basal insertion point of the right coronary cusp (white arrowhead).



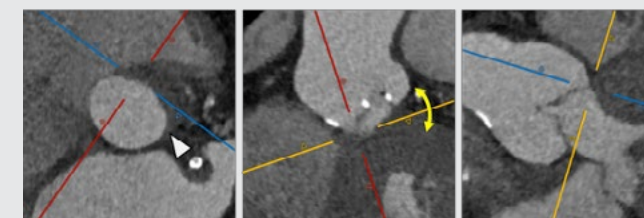
Step 4

Rotate the crosshairs counterclockwise without moving up and down while maintaining its center position so that the formerly coronal view (here red crosshair) transects the lowest insertion point of the non-coronary cusp, which is located at approximately 8 o'clock (white arrowhead).



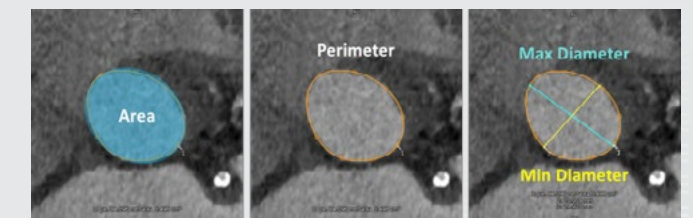
Step 5

The formerly coronal, now double-oblique transverse, view will show the lowest insertion point both of the right coronary cusp and the non-coronary cusp (white arrowheads). In this view, rotate the (here orange) crosshair indicating the double-oblique transverse view to transect exactly through the most basal insertion point of the non-coronary cusps. Once this is achieved, the double-oblique transverse plane will contain two of the three lowest cusp insertion points.



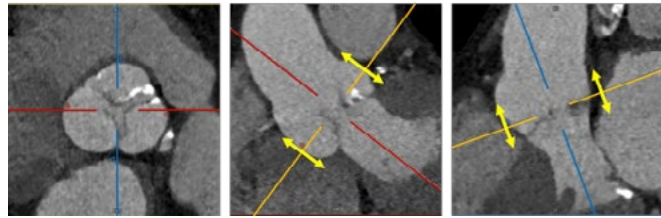
Step 6

In the formerly sagittal view, rotate (without moving it) the crosshair of the double-oblique transverse plane (here orange) until the lowest insertion point of the left coronary cusp just barely appears in the double-oblique transverse view (white arrowhead). Now, the formerly axial plane is exactly aligned with the lowest cusp insertion points of all three aortic cusps and represents both the orientation, as well as the level of the annular plane.

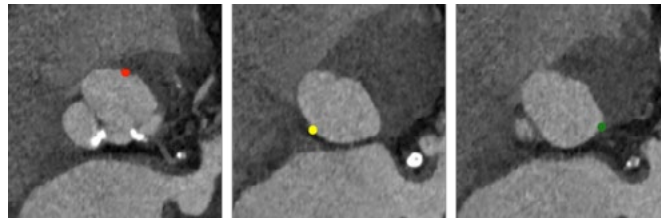


Step 7

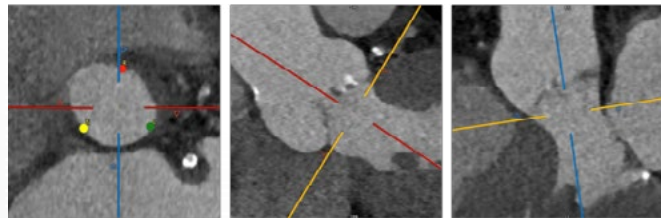
Measurements of aortic annulus dimensions should be performed in the annular plane by means of a contouring tool.



Start out with multiplanar images, or center-line technique, aligned with the aortic valve. Move up and down (yellow arrows) along the aortic root to identify most basal hinge points.



Identify and mark most basal hinge points of the right coronary cusp (red dot), non-coronary cusp (yellow dot), and left coronary cusp (green dot).



Software automatically identifies and displays annular plane defined by the previously identified three most basal hinge points.

Figure 11. Facilitated annular segmentation.

Note:

Confirmation of the correct identification of the annular plane is warranted for both the facilitated and semi-automated segmentation, ie, by “turning” the crosshairs and verifying the location of the hinge points on the long axis view.

Facilitated Annular Segmentation

Certain post-processing platforms facilitate annular segmentation by manual placement of seeding points at the identified hinge points. After placing a seeding point for each of the three cusps, the plane transecting all three points is automatically displayed (FIGURE 11).

Semi-automated Annular Segmentation

Certain post-processing platforms perform an automated segmentation of anatomical landmarks, including the basal hinge points, allowing for an automated display of the annular plane. If these techniques are employed, the displayed contour should be manually validated and corrected if necessary.

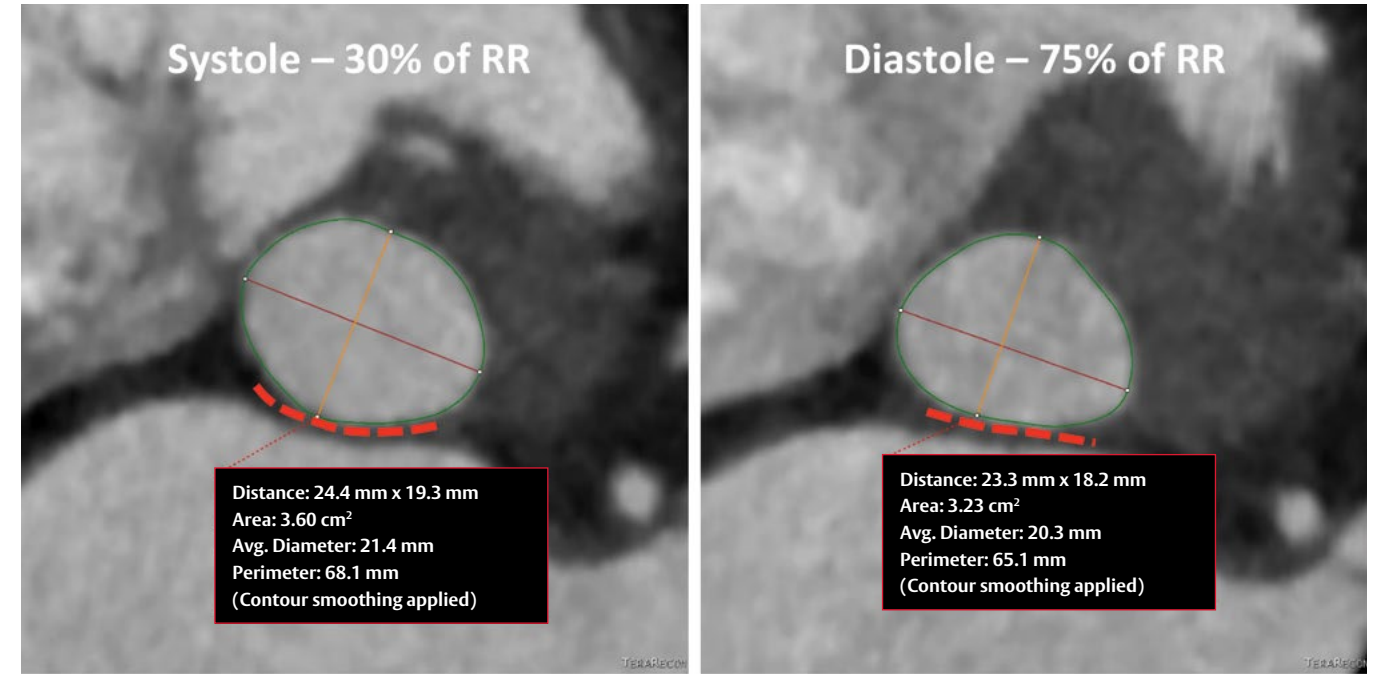
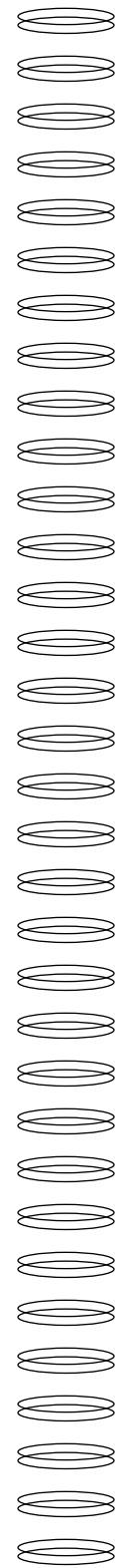


Figure 12. Dynamic changes in annular dimensions and configuration throughout the cardiac cycle. Conformational changes occur due to bulging of the aorto-mitral junction (red dashes) toward the left atrium during systole.

Importance of Cardiac Phase for Determining Maximum Aortic Annular Dimensions

- The aortic annulus is subject to pulsatile and deformational changes throughout the cardiac cycle.
- The annular area may vary greatly between systole and diastole (FIGURE 12). Edwards sizing charts are based on maximum systolic area. Maximum systolic area is determined by manually evaluating available image reconstructions.
- Assessment of annular dimensions should not be limited to prespecified phases only (eg, 35%) as the phase with largest dimensions varies amongst patients.

Annular and Aortic Root Measurements

After proper identification of the annular plane, the annulus measurement and ancillary measurements should be performed.

These measurements can be grouped dependent on the annular plane and independent of the annular plane.

It is recommended to perform the assessment in the following sequence:

1. Identify the annular plane.
2. Perform measurements dependent on the annular plane.
3. Perform measurements independent of the annular plane.

Although several automated tools are commercially available to expedite the valve analysis workflow, it is important to understand the approach for each measurement in order to be capable of performing the assessment manually and to recognize errors that may occur in an automated analysis.

Measurements Dependent on the Annular Plane:

- Annular dimensions
- Prediction of fluoroscopic angulation
- Distance to coronary ostia (coronary artery height)
- Sinotubular junction (STJ) height
- Left ventricular outflow tract (LVOT)
- Ascending aorta length

Measurements Independent of Annular Plane:

- Sinus of Valsalva width
- Sinotubular junction (STJ) diameter
- Ascending aorta diameter

The annular assessment and measurements are used with additional imaging modalities, as well as patient characteristics, to determine the appropriate prosthesis size.

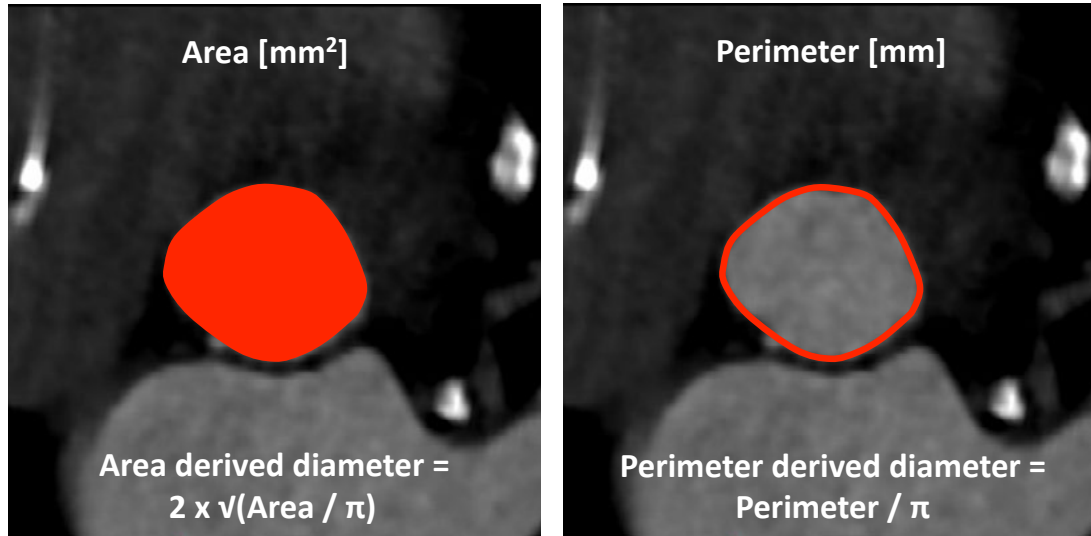


Figure 13. Various descriptors of annular dimensions.

Annular Dimensions

In general, annular dimensions (FIGURE 13) can be expressed in the following terms:

- Area
- Diameter
- Perimeter

It is important to understand that a **diameter** can be measured using an electronic caliper (simple distance measurement tool) and derived from perimeter or area using a mathematical equation.

Area and **perimeter** are planimetrically assessed by utilizing manual contouring, a spline (explained below), or a semi-automated contour with contrast-edge detection.

The aortic annulus is usually elliptical. A simple distance measurement, such as a long axis or short axis distance, does not integrate the rather complex dimensions of an ellipse and is subject to greater measurement error.

Caliper measurements to assess short- and long-axis dimensions can be used to describe the ellipticity but have limited value for annular sizing.

Some post-processing platforms provide maximum diameter (long axis) and minimum diameter (short axis) based on annular planimetry. However, there is no standardization across post-processing platforms as to how these diameters are defined.

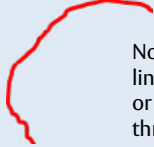
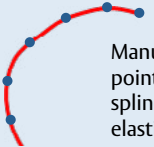
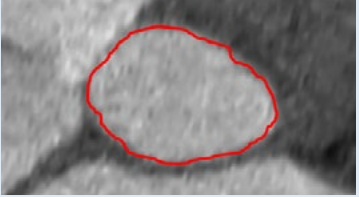
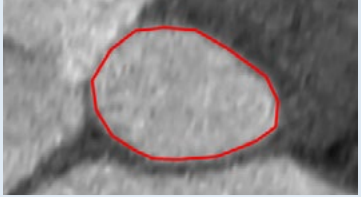
Freehand tool or Hounsfield-based contour detection	Polygon	Spline
 <p>Non-smoothened, irregular line following path of cursor or detected attenuation threshold</p>	 <p>Manually placed segmentation points connected by straight line without interpolation</p>	 <p>Manually placed segmentation points connected by a cubic spline interpolation – elastic ruler</p>
 <p>Systematic overestimation of perimeter due to non-smoothened contour; smoothing algorithms can allow for more realistic perimeter assessment.</p>	 <p>Depending on the number of dots, this may yield a closer estimate of perimeter than freehand contouring without smoothing.</p>	 <p>Accurate quantification of annular perimeter.</p>

Table 2. Methods for performing planimetry.

Planimetry is performed by one of the following methods:

- Manual contouring
 - ~ Freehand tool
 - ~ Polygon tool
 - ~ Spline tool
- Semi-automated, Hounsfield unit-based edge detection

Independent of the approach, planimetry yields an **area** commonly expressed as mm² or cm². The area measurement can be used to calculate an effective area-derived diameter using the formula listed in FIGURE 13. Most advanced post-processing tools perform this calculation automatically. However, current Edwards sizing charts list the source values (area, perimeter) and do not require the user to derive an effective diameter.

A freehand contour of the region of interest follows the path of the cursor while a polygon is created by placing dots along the annular contour, which

are automatically connected without interpolation. In contrast, a **spline** tool is similar to an elastic ruler that bends to pass through the manually defined points.

Depending on the vendor, these planimetry tools may also yield **perimeter values**. However, a freehand contour often results in an irregular line, which leads to an artificially increased perimeter. Polygons and splines usually have a smooth contour, yielding a more realistic perimeter value. Smoothing algorithms can allow for perimeter assessment using freehand contours by correcting the jagged contour.

Edge-detection algorithms help identify the annular contour based on the edge between the contrast-attenuated lumen and the non-enhancing mural components. Importantly, automatically drawn contours should be visually validated and, if necessary, manually corrected. Also, smoothing algorithms should be applied, if the perimeter value is used for prosthesis sizing.

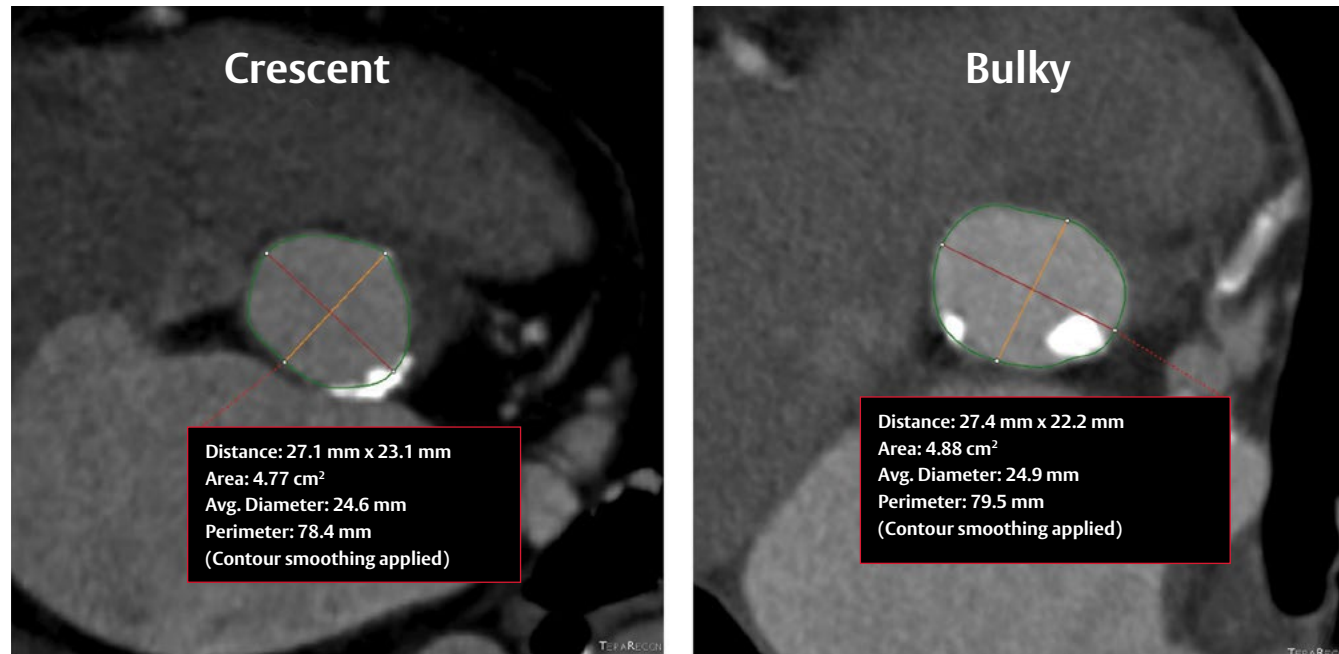


Figure 14. Annular assessment in the presence of annular calcifications.

Annular Dimensions in the Presence of Annular Calcifications

Annular calcifications can be classified as:

- Adherent (crescent)
- Protruding (bulky)

The annular contour should be traced, extrapolating as if the calcification were not present (FIGURE 14).

It is important to also assess the entire anticipated landing zone for the presence of calcifications, for example, at the level of the annulus, subannular region (0 to 2 mm below annulus), and the upper LVOT (determined by planned depth of implant).

Prosthesis sizing should take into account calcium distribution, location, and size.

Prediction of Fluoroscopic Angulation:

- Fluoroscopic angulation required to achieve a coplanar fluoroscopic view of the aortic annulus can be obtained prior to the procedure from the CT data set.
- This may help reduce the number of aortograms needed in order to achieve an acceptable view at the time of the procedure, thus decreasing the volume of contrast material being used.
- Most post-processing platforms report the angulation of each of the three views of the MPR as pairs of degrees [°] LAO/RAO and CRA/CAU angulation (FIGURE 15A).
- These angulations are located on the patient-specific optimal viewing curve (FIGURE 15B).

Step 1

Following the annular measurement, DO NOT change the angulation or level of the annular plane (double-oblique transverse image) (FIGURE 15A).

Step 2

By rotating the crosshairs in the oblique transverse view, the orientation of the coronal double-oblique view is moved along the optimal viewing curve, which is reflected by a change in the displayed values for °LAO/RAO and °CRA/CAU angulation.

- For example, if the implanter prefers a view with 0° CRA/CAU angulation, the coronal view is adjusted to 0° CRA/CAU angulation and the corresponding LAO angulation is noted.
- Common angulation pairs include the following:
 - 10° LAO, corresponding CRA/CAU angulation
 - 0° LAO/RAO, corresponding CRA/CAU angulation
 - 30° LAO, corresponding CRA/CAU angulation
 - 0° CRA/CAU, corresponding LAO/RAO angulation

Accuracy of the derived C-arm angulation is dependent on the patient being positioned on the CT table in a similar fashion as in the cath lab.

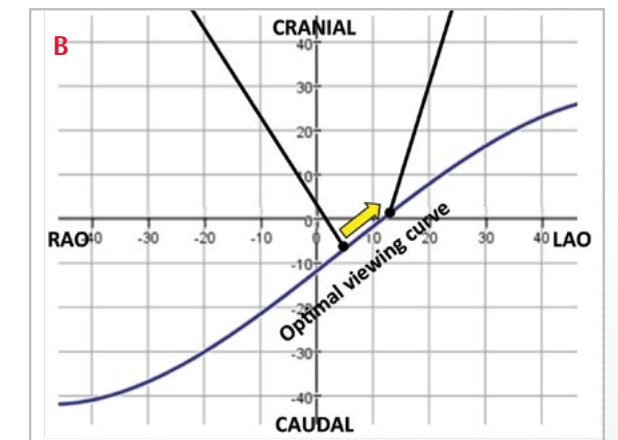
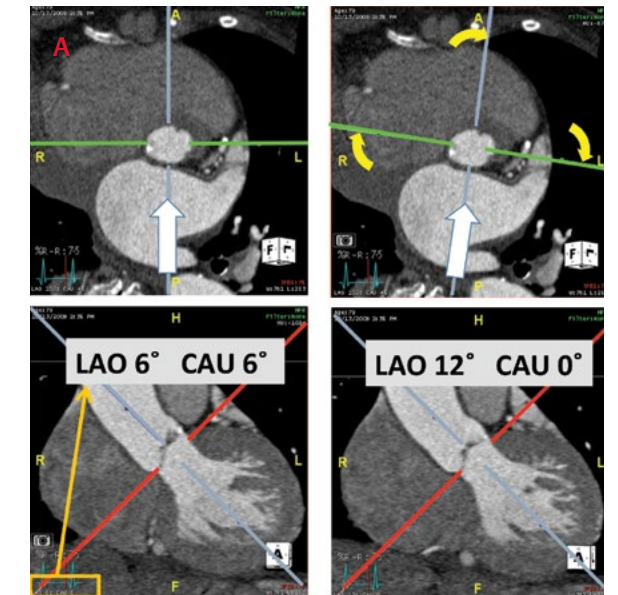


Figure 15. Required pairs of LAO/RAO and CRA/CAU angulation to achieve a coplanar view of the aortic annulus are located on the patient-specific optimal viewing curve.

Fluoroscopic View With Right Cusp Centered

The interventionalist may prefer a coplanar fluoroscopic view with the right cusp centered between the non-coronary cusp and the left coronary cusp. This view can be simulated by rotating the crosshairs on the annular plane (double-oblique transverse view) (FIGURE 16).

- The crosshairs have to remain centered within the annular contour.
- The crosshair indicating the orientation of the sagittal double-oblique plane is rotated to bisect the right coronary cusp/transsect through the most basal hinge point of the right coronary cusp.

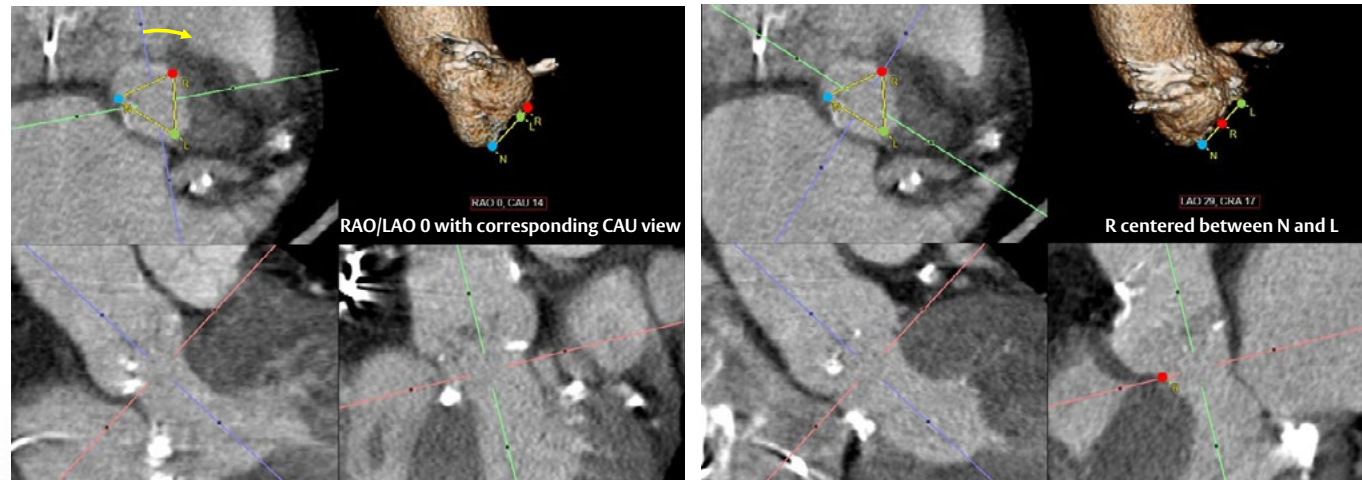


Figure 16. By rotating the crosshairs on the double-oblique transverse view (annular plane view, yellow arrow) to transect the right coronary cusp hinge point (R), the orientation of the coronal double-oblique coronal view is adjusted to center R between the non-coronary and left coronary cusp hinge points (N and L).

Coronary Artery Height

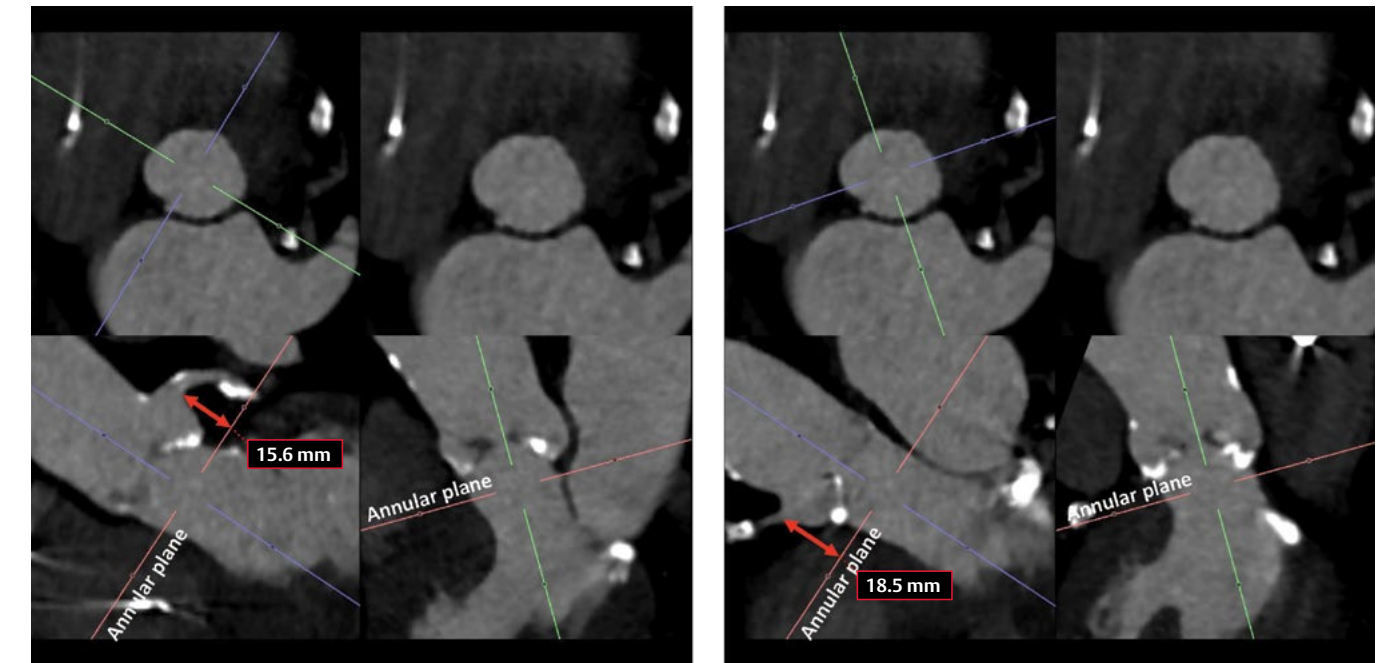


Figure 17. Assessment of coronary artery height.

The distance from the annular plane to the coronary ostia is critical to identify patients with low coronary height and increased anatomical risk of coronary occlusion. The prosthesis may displace the native leaflets and/or calcium, thereby potentially occluding the ostium.

Step 1

Following the annular measurement and fluoroscopy angulation assessment, do NOT change the angulation or level of the annular plane (double-oblique transverse image).

Step 2

By spinning the crosshairs on the oblique transverse view, adjust so that the double-oblique coronal view transects the left main ostium.

Step 3

Measure the vertical height from the annular plane to the inferior aspect of the left coronary ostia, perpendicular to the annular plane, as shown in the image above (FIGURE 17).

Step 4

Repeat steps 1 to 3 for the right coronary ostia.

Sinus Height/Sinotubular Junction Height

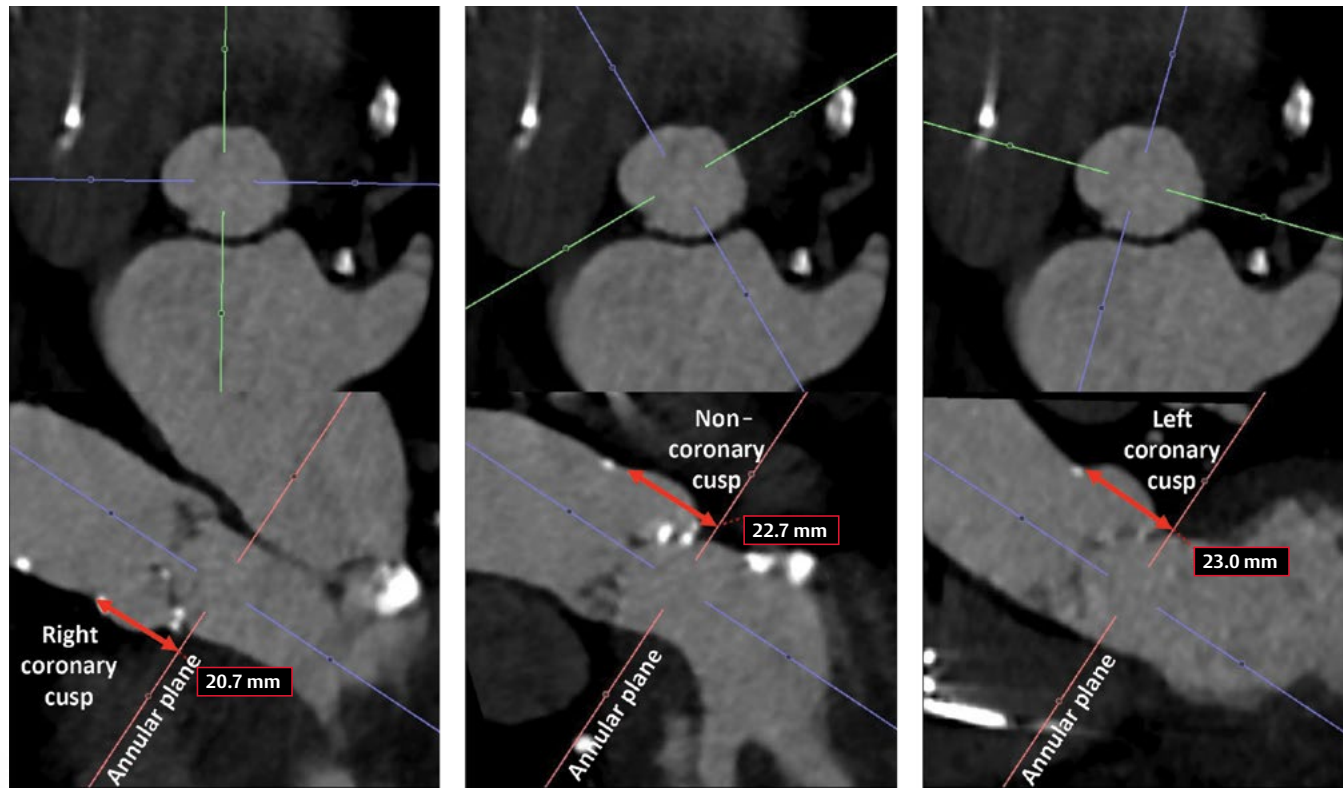


Figure 18. Assessment of sinus/STJ height.

The STJ height is critical in a case of high implantation in which the prosthesis may come into contact with the STJ.

Step 1

Do NOT change the angulation or level of the annular plane (double-oblique transverse image).

Step 2

By spinning the crosshairs on the oblique transverse view, adjust so that the double-oblique coronal view transects the center of the desired cusp (eg, right coronary cusp).

Step 3

Measure the vertical height from the annular plane to the STJ, perpendicular to the annular plane, as shown in the image above (FIGURE 18).

Left Ventricular Outflow Tract (LVOT)

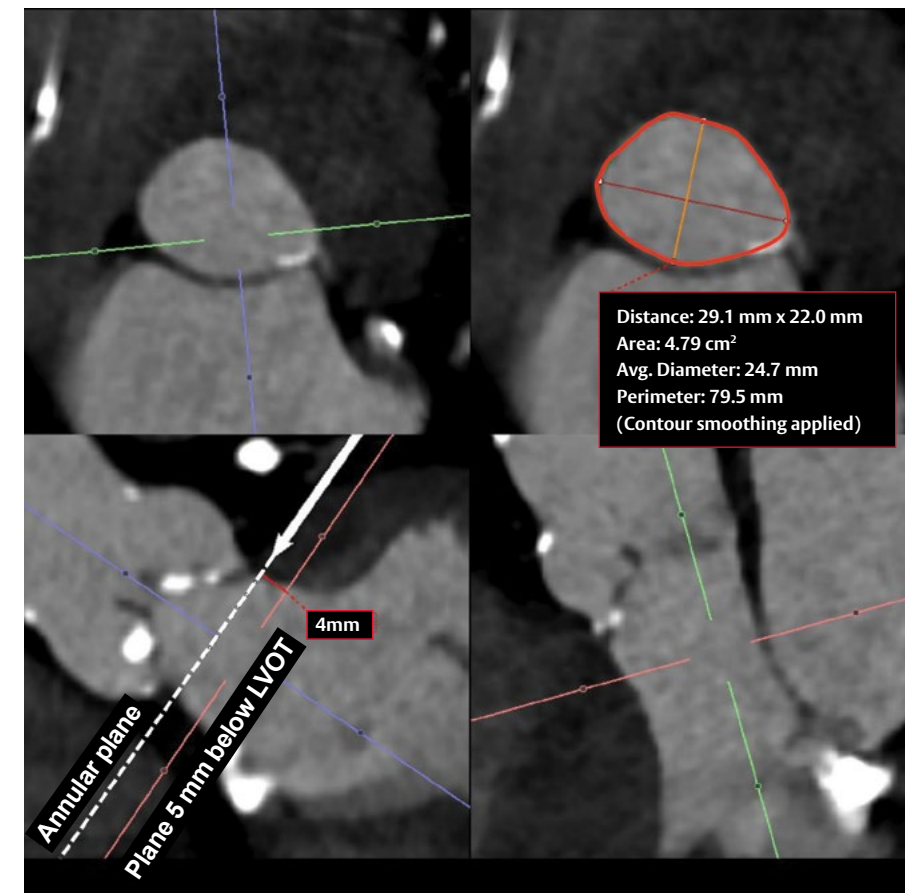


Figure 19. Assessment of LVOT area 4 mm below annular plane.

It is important to assess the LVOT for the presence and distribution of calcium. In addition, LVOT planimetry informs LVOT geometry (FIGURE 19):

- ~ Funnel-shaped LVOT, with LVOT > annular dimensions; most pronounced in the setting of a dilated left ventricle
- ~ Tapering LVOT, with LVOT < annular dimensions; most pronounced in the setting of septal hypertrophy

Step 1

Do NOT change the angulation or level of the annular plane (double-oblique transverse image).

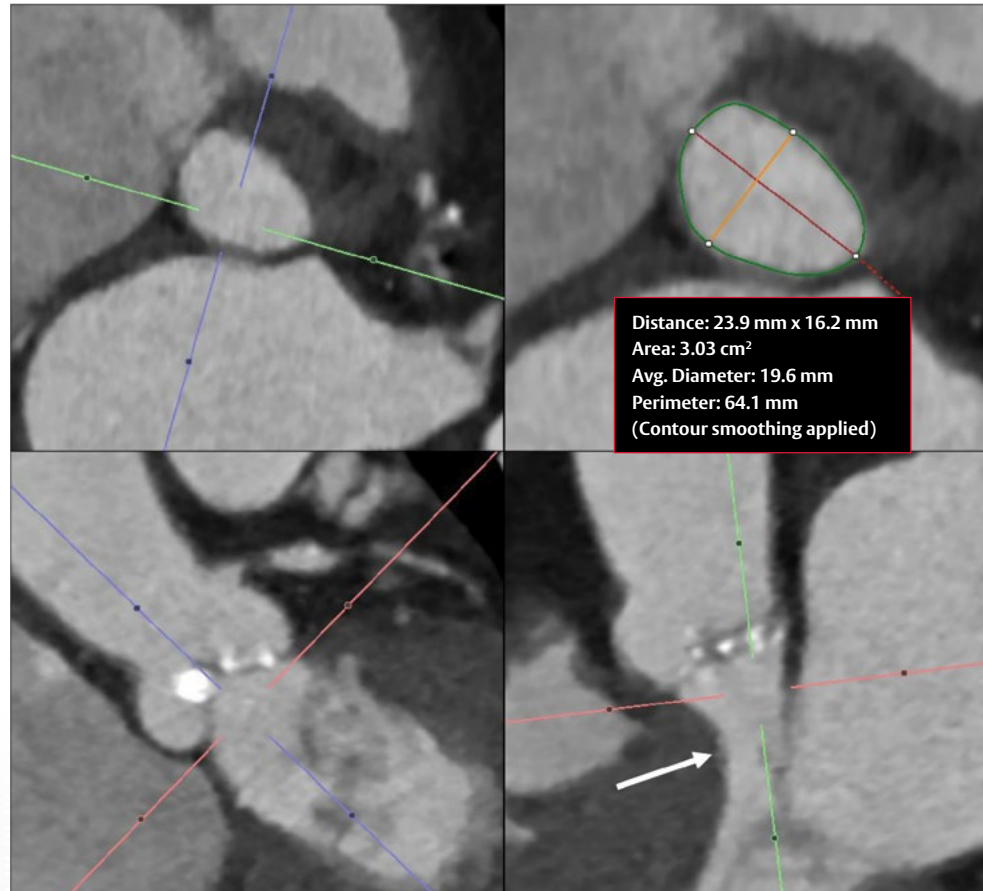


Figure 20. Pronounced septal bulge (white arrow).

Step 2

Change the level of the double-oblique transverse plane 4 mm into the LVOT without changing its orientation (FIGURE 19).

- Assess the LVOT area by means of planimetry or measure the maximum and minimum diameters.
- The LVOT anatomy should be assessed for the presence of a septal bulge (FIGURE 20).

Sinus of Valsalva Width

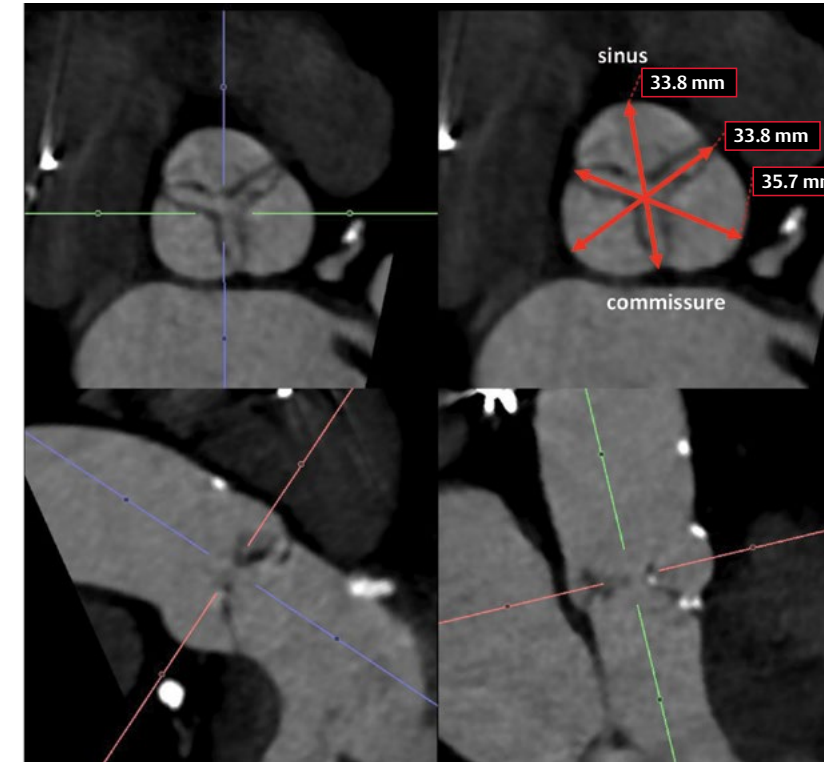


Figure 21. Assessment of sinus of Valsalva dimensions.

The sinus width is important to assess for shallow, noncapacious sinuses. Non-capacious sinuses may predispose to coronary occlusion.

Step 1

Change the level of the double-oblique transverse view (annular plane) toward the sinus of Valsalva, usually by scrolling until you reach the widest portion of the sinus of Valsalva.

Step 2

Measure the distance from the left coronary sinus to the opposing commissure using a distance measurement tool (FIGURE 21).

Step 3

Repeat for the right coronary sinus and the non-coronary sinus, always measuring to the opposing commissure.

Step 4

Average all three values by adding them and dividing by three.

Sinotubular Junction (STJ) Diameter

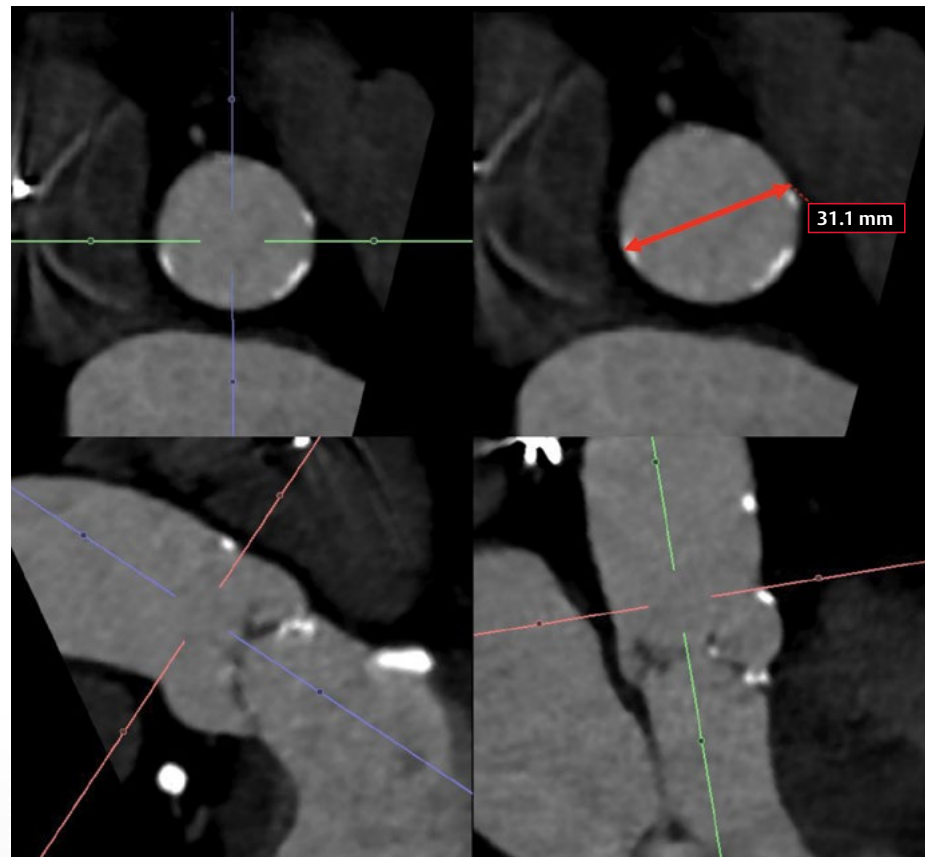


Figure 22. Assessment of STJ diameter.

The STJ diameter is critical in a case of high implantation in which the prosthesis may come into contact with the STJ.

Step 1

Change the level of the double-oblique transverse view toward the STJ; the angulation may have to be changed.

Step 2

Identify the STJ, and measure the diameter using the distance measurement tool (FIGURE 22).

Ascending Aorta Diameter

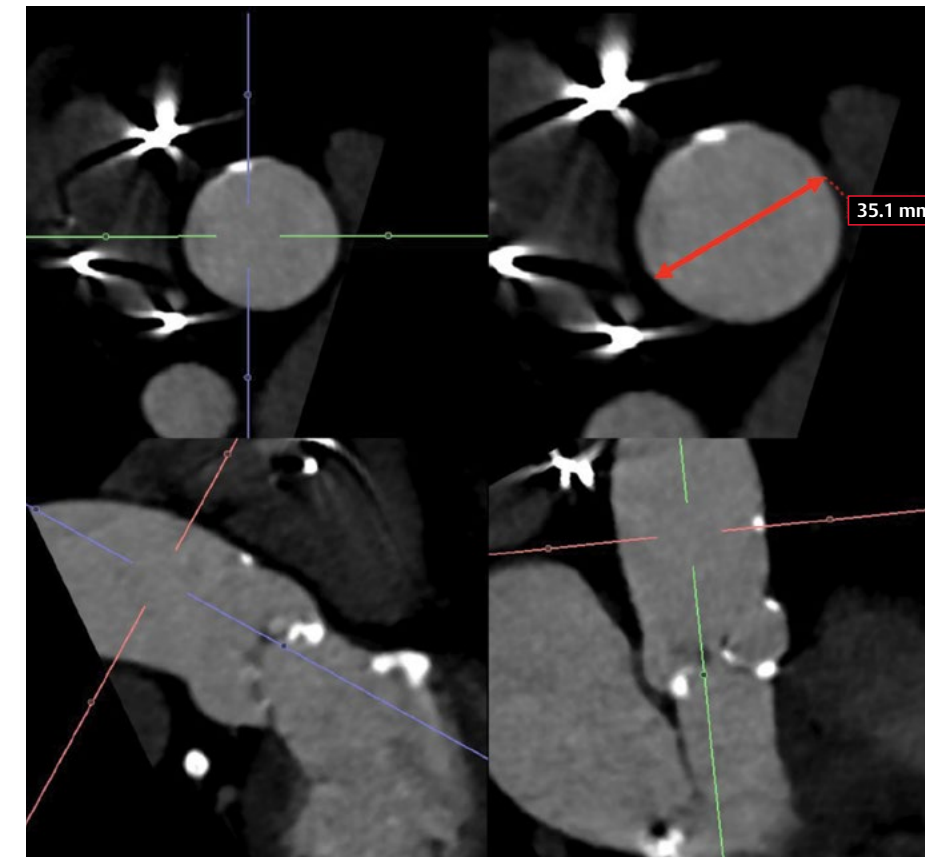


Figure 23. Assessment of ascending aortic diameter.

The ascending aorta diameter is important to evaluate for the presence of an ascending aortic aneurysm.

Step 1

Change the level of the transverse double-oblique view toward the ascending aorta. The angulation has to be changed so that the double-oblique transverse view transects the ascending aorta perpendicular to its long axis (usually resulting in a circular shape of the ascending aorta on the transverse view).

Step 2

Measure the diameter using the distance measurement tool. The measurement should be performed approximately 4 cm above the annular plane, or at the level of the greatest width (FIGURE 23).

Pre-procedural Assessment for Aortic Valve-in-Valve Procedures

Aortic valve-in-valve (aViV) implantation of a transcatheter heart valve into a failed bioprosthetic heart valve has emerged as a treatment alternative to repeat conventional surgery. This requires careful pre-procedural assessment using noninvasive imaging to identify patients at risk for procedure-related adverse events, such as coronary obstruction.

For aViV, a pre-procedural CT is required to:

- Assess the anatomical risk of coronary obstruction
- Assess an access route for the procedure (see section on access)

In certain instances, CT can also facilitate to:

- Determine the bioprosthetic valve type
- Determine the bioprosthetic valve size
- Determine the appropriate fluoroscopic projection

Requirements for CT Data Acquisition and Reconstruction. In general, CT imaging requirements are similar to the requirements for planning of transcatheter aortic valve implantation for native aortic stenosis.

Recommendations – CT Data Acquisition and Reconstruction:

- Acquire contrast-enhanced, ECG-synchronized CT data of the aortic root covering the entire cardiac cycle.
- Use the recommended ECG-assisted acquisition technique for scanner system used (see section on acquisition).
- Consider ECG-synchronized, thin-sliced non-contrast cardiac CT in case of contraindication for intravenous contrast agent.

- Contrast-enhanced, ECG-synchronized cardiac CT data set covering at least the aortic root. Although the lack of dynamism (rigid bioprosthetic heart valve scaffold) would theoretically require only one cardiac phase, acquisition and reconstruction of the entire cardiac cycle allows for abundant CT data, which may be beneficial in case of artifacts.
- Higher tube voltage (eg, 140 kVp) can help reduce beam-hardening artifacts and metal blooming, when compared to standard tube voltage (such as 100 or 120 kVp).
- Noncontrast CT data sets may be sufficient for assessment of coronary obstruction risk, as coronary artery orifices can be identified based on surrounding epicardial fatty tissue. However, acquired CT data must be ECG-synchronized and thin-sliced (not to be mistaken with thick-sliced coronary artery calcium scoring CT). This applies to stented bioprosthetic valves (rigid scaffold), but not to stentless valves.

Prediction of Risk of Coronary Obstruction

Coronary obstruction in aViV is caused by a bioprosthetic leaflet that is being displaced outward into open position by the transcatheter heart valve, thereby forming a membrane-covered cylinder, which may be coming in direct, or near-direct, contact with a coronary ostium. Importantly, obstruction may also occur above the coronary ostium when the created membrane-covered cylinder is in close proximity to the sinus wall.

- The distance of the membrane-covered cylinder and the coronary ostia/sinus wall determines the patient-specific risk of coronary obstruction.
- The distance itself is determined by:
 1. Root anatomy (in particular the width)
 2. Degree and orientation of bioprosthetic heart valve canting, as the scaffold of the bioprosthetic heart valve will determine the orientation of the transcatheter heart valve and thus the membrane covered cylinder

For this reason, assessment of the risk of coronary obstruction requires simulation by virtual implantation of the transcatheter heart valve with subsequent measurement of the anticipated distance to the coronary ostium (**FIGURE 24**). This measurement is referred to as *virtual THV to coronary distance* (VTC). Measurements performed above the ostium toward the sinus wall are referred to as *virtual THV to sinus distance* (VST).

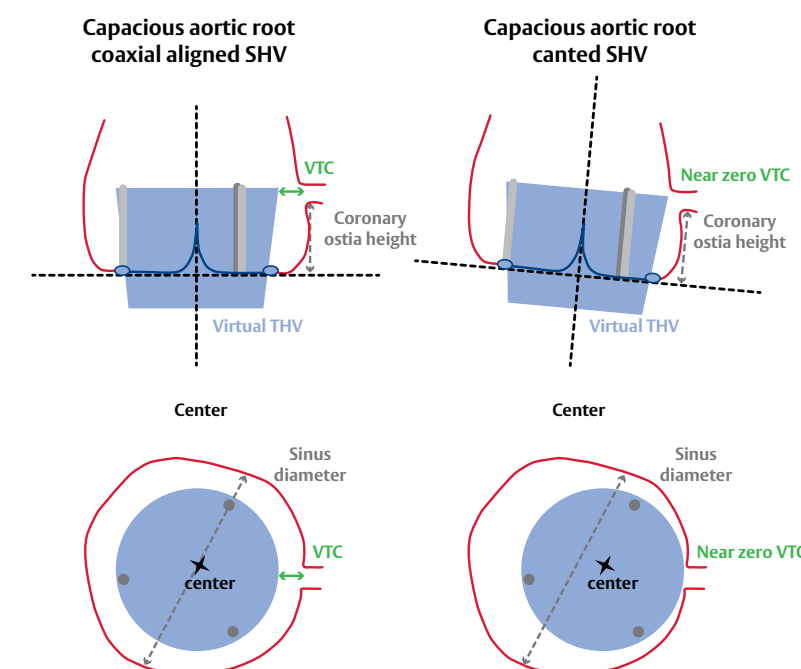


Figure 24. Importance of assessment of the virtual THV to coronary distance (VTC) to account for canting of the surgical valve in an overall spacious aortic root.

Practical Considerations for VTC Assessment

In general, VTC assessment should be performed in patients who are at risk, ie, if:

- Coronary arteries arise at the level of the bioprosthetic heart valve (ie, below the tip of the posts).

No further VTC analysis is needed if: (FIGURE 25)

- Coronary arteries arise above the tip of the posts.
- Patient is status post CABG with complete revascularization and patent grafts.

In patients with stentless bioprosthetic heart valves, root analysis should be performed in a similar fashion to

native aortic stenosis, as a stentless valve will less likely determine the final orientation of the transcatheter heart valve due to the lack of a rigid scaffold.

VTC assessment can be performed with:

- Multiplanar reformats (MPRs) using a circular region of interest tool (ROI) to simulate the expanded THV (FIGURE 26).
- Dedicated post-processing software allowing to virtually implant a cylinder simulating the expanded THV.

It is important to reference the device IFU in order to obtain the device-specific dimensions utilized in virtual implants.

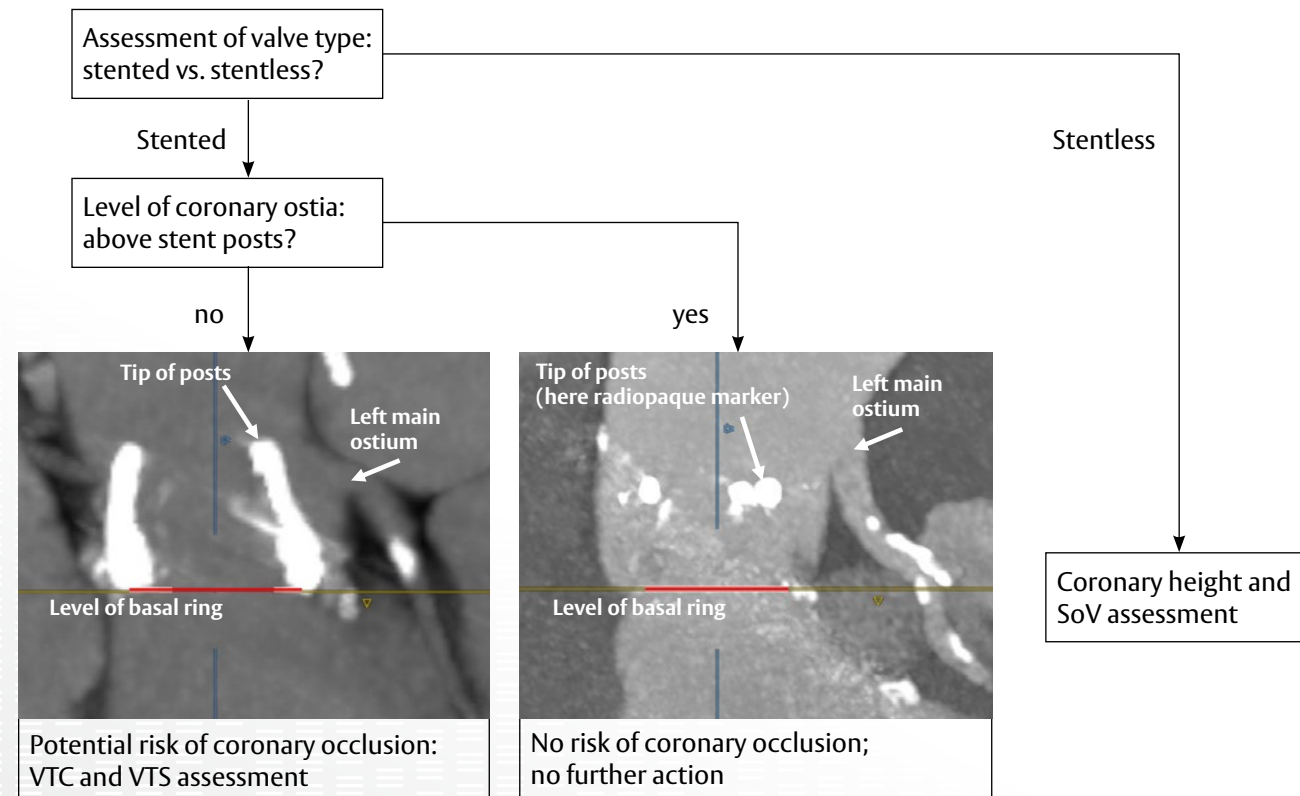


Figure 25. Stepwise approach to understanding individualized risk of coronary occlusion.



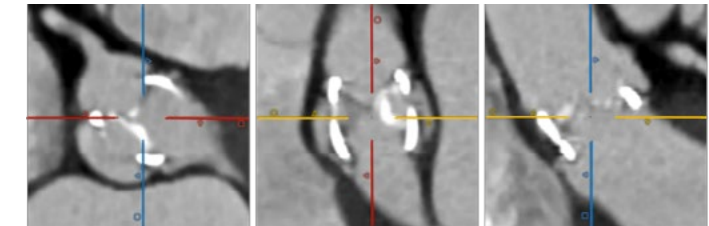
Step 1

Identify surgical heart valve type, eg, using a volume-rendered reconstruction.



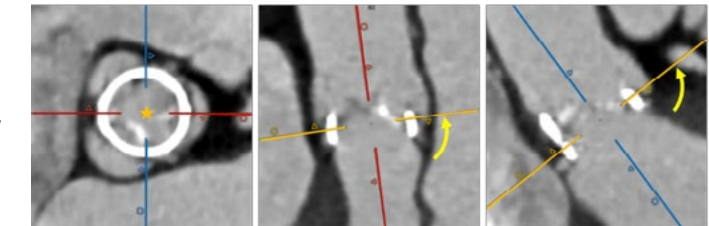
Step 2

Center crosshairs within the surgical heart valve.



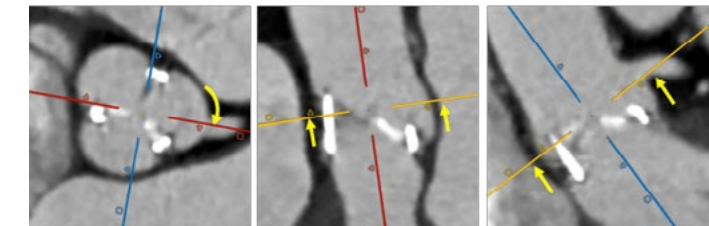
Step 3

Manipulate crosshairs so that the double-oblique transverse plane is aligned with the sewing ring of the surgical heart valve. **Note:** In some valves with nonplanar/noncontiguous radiopaque sewing ring, only the three most basal portions of the sewing ring should be visible. Center the crosshairs in the center of the sewing ring (asterisk).



Step 4

Move the double-oblique plane to the level of the coronary ostium (yellow arrows), without changing the orientation/angulation; then rotate the crosshairs on the double-oblique view to align with the coronary ostium (here left main ostium).



Step 5

Simulate the transcatheter heart valve using a circular region of interest (dashed green circle) with its center aligned with the center of the surgical heart valve/ crosshairs. The region of interest should represent the size of the anticipated transcatheter heart valve. Measure the distance (VTC) from the circle to the coronary orifice (here left main).

Repeat for right coronary artery.

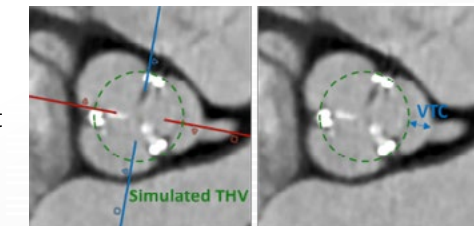


Figure 26. Workflow for prediction of anatomical risk of coronary artery obstruction in ViV procedures depending on valve type and level of coronary artery orifices. For stented SHVs, VTC assessment is required only if the coronary artery orifices are located at or below the tip of the stent posts. For sutureless SHVs, a traditional coronary height/SoV-width assessment is performed.

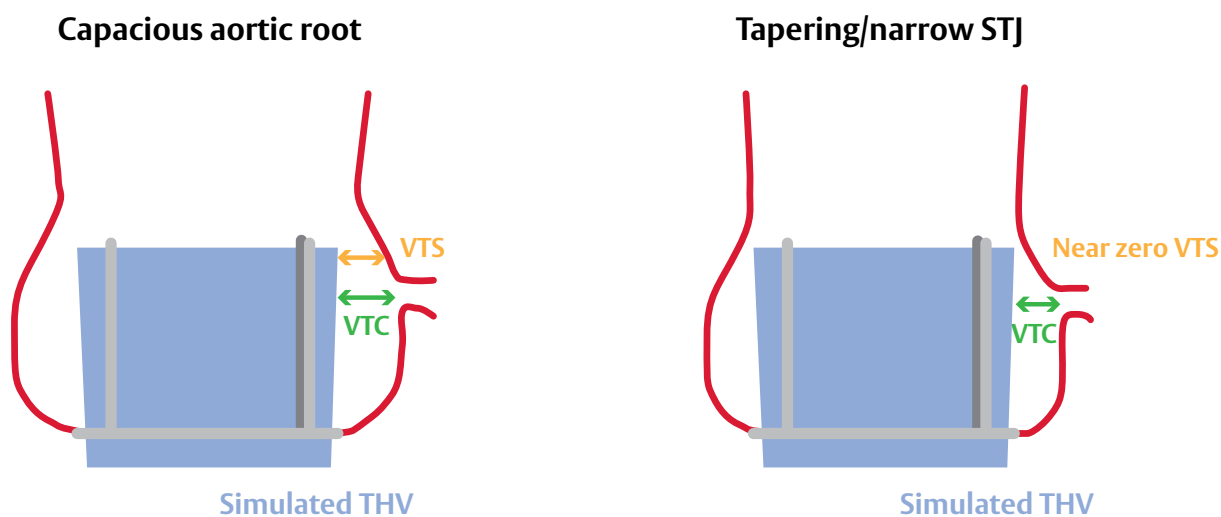


Figure 27. While the VTC refers to the virtual distance between anticipated THV and coronary ostium, the VTS refers to the distance to the sinus wall above the ostium, if the surgical bioprosthesis extends that high. In patients with narrow roots, the VTS can be significantly reduced, despite the VTC being sufficient, harboring the risk of sinus sequestration.

Interpretation of VTC and Other Measurements:

- The determined VTC and the distance to the STJ (if applicable) are the most important measurement values to determine the patient-specific risk of coronary obstruction.
- Coronary height and SOV width measurements have less predictive capabilities.
- A VTC <4 mm indicates a higher risk of obstruction.
- Importantly, VTC measurements should not be limited to the level of the coronary ostia. The relationship of the anticipated transcatheter heart valve to the sinus wall and STJ above the ostium should be assessed, in particular, if the surgical bioprosthesis reaches the STJ.

These measurements are being referred to as Virtual THV to sinus distance (VTS) (FIGURE 27).

Other considerations:

- Similarly to fluoroscopy, CT imaging can aid in determining the bioprosthetic heart valve present in case of unknown surgical history. Appearance of the sewing ring and posts with radiopaque and non-radiopaque components is usually unique for a certain valve type.
- While CT allows for measuring of bioprosthetic heart valve dimensions, derived values depend on measurement technique and image quality (ie, metal blooming) and do not resemble established stent internal diameter or true internal diameter.

Pre-procedural Assessment for Mitral Valve-in-Valve Procedures

Mitral valve-in-valve (mViV) implantation of a transcatheter heart valve into a failed bioprosthetic heart valve has emerged as a treatment alternative to repeat conventional surgical valve replacement. This requires careful pre-procedural assessment using noninvasive imaging to identify patients at risk for procedure-related adverse events, such as left ventricular outflow tract obstruction (LVOTO).

For mViV, a pre-procedural CT is required to:

- Assess the anatomical risk of LVOTO
- Assess an access route for procedure (see **Chapter 5** for trans-septal access, or transapical)

In certain instances, CT can also facilitate to:

- Determine the bioprosthetic valve type
- Determine the bioprosthetic valve size
- Determine appropriate fluoroscopic projection

Requirements for CT data acquisition and reconstruction. In general, cardiac CT imaging requirements are similar to the requirements for planning of transcatheter aortic valve implantation for native aortic stenosis except that it does not require acquisition of CT data of the abdomen and pelvis.

- Contrast-enhanced, ECG-synchronized cardiac CT data set covering the entire heart throughout the entire cardiac cycle.
- Data of the entire cardiac cycle is needed due to expected variations in LVOT dimensions throughout systole and diastole.
- Higher tube voltage (eg, 140 kVp) can help reduce beam-hardening artifacts and metal blooming, when compared to standard tube voltage (such as 100 or 120 kVp).

Recommendations – CT Data Acquisition and Reconstruction:

- Acquire contrast-enhanced, ECG-synchronized CT data of the entire heart, covering the entire cardiac cycle.
- Use recommended ECG-synchronized acquisition technique for scanner system used (see **TABLE 1, page 8**).

Mechanism of LVOT Obstruction in mViV

In mViV, a transcatheter heart valve is placed into the failed bioprosthetic surgical valve, thereby displacing the bioprosthetic leaflets into the open position and creating a membrane-covered cylinder. This membrane-covered cylinder may encroach upon the native LVOT, potentially resulting in an insufficient outflow tract. The altered LVOT is commonly referred to as neo-LVOT. Neo-LVOT dimensions are multifactorial, including patient anatomy such as LV size, septal dimensions, and aortomitral angulation as well as the characteristics of the bioprosthetic surgical valve.

Assessment of Anticipated Neo-LVOT Dimensions

The complex, multifactorial relationship between native anatomy and the membrane-covered

cylinder being created requires simulation by virtual implantation of the transcatheter heart valve with subsequent measurement of the anticipated neo-LVOT dimensions. This assessment can be performed using dedicated post-processing software.

Practical Considerations

Prediction of neo-LVOT dimensions follows a stepwise workflow (see **Figure 28** below):

1. Segmentation of the bioprosthetic surgical valve.
2. Simulation of the transcatheter heart valve (virtual implant).
3. Segmentation of the neo-LVOT.
4. Assessment of the neo-LVOT cross-sectional area.

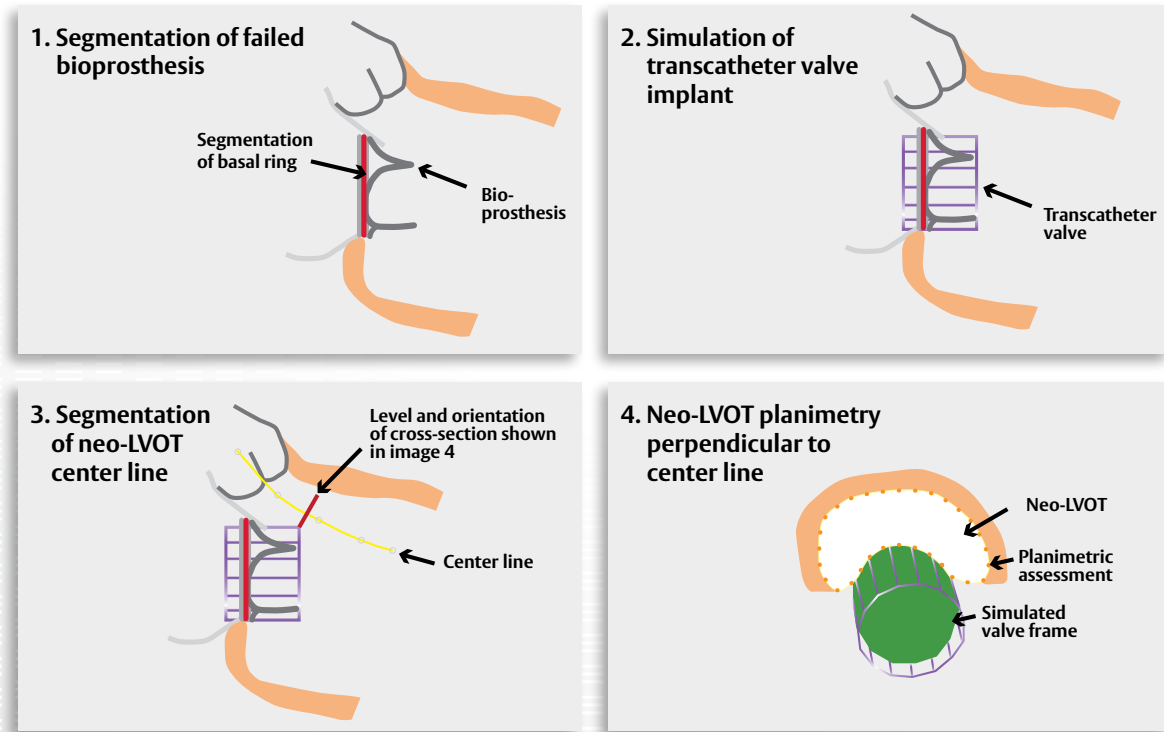


Figure 28. Schematic illustration of neo-LVOT segmentation for assessment of potential LVOT obstruction.

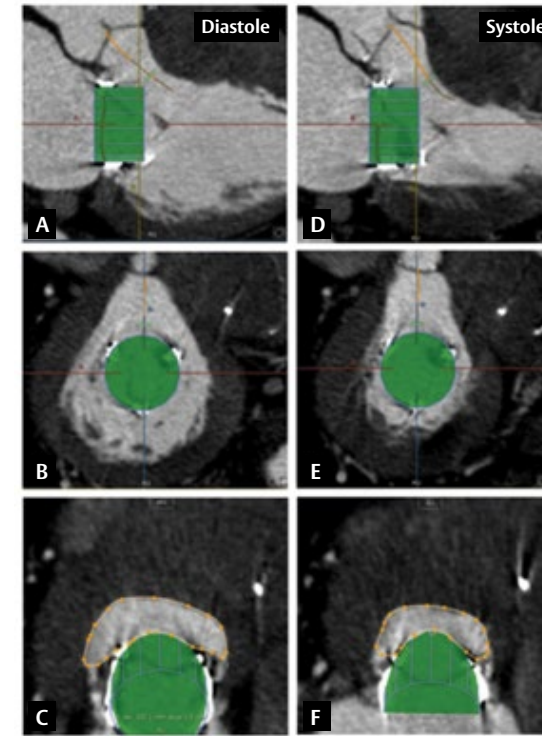


Figure 29. Example of LVOT segmentation at end-diastole and end-systole in a patient prior to mViV.

- Assessment should be performed at end-systole when neo-LVOT dimensions are smallest. Additional assessment in other phases can inform the dynamic changes throughout the cardiac cycle (**FIGURE 29**).
- The simulated transcatheter heart valve should reach the tip of the posts. This is critical, as this accounts for the bioprosthetic leaflets in open position independent of the level of final transcatheter heart valve positioning. **Note:** For implant positioning, please refer to the IFUs.

Other Considerations

- Similarly to fluoroscopy, CT imaging can aid in determining the bioprosthetic heart valve present in case of unknown surgical history. Appearance of the sewing ring and posts with radiopaque and non-radiopaque components are usually unique for a certain valve type.
- While CT allows for measuring of bioprosthetic heart valve dimensions, derived values depend on measurement technique and image quality (ie, metal blooming) and do not resemble established stent internal diameter or true internal diameter.

Bicuspid Aortic Valve

Bicuspid aortic valves are the most common congenital cardiac abnormalities. While bicuspid valve morphology constitutes a predisposing factor for the development of aortic stenosis, valve morphology has to be accounted for when planning transcatheter aortic valve procedures. Accurate anatomical knowledge of valve morphology is, therefore, critical to procedural success. CT imaging has proven to be a useful imaging modality for identifying patients' valve and root morphology prior to transcatheter aortic valve procedures.

Procedural planning of transcatheter aortic valve procedures includes the following:

- Determining the aortic valve morphology
 - ~ Valve configuration
 - ~ Valve and/or raphe calcification
- Assessing aortic annular geometry and dimensions
- Assessing aortic root and ascending aorta morphology

As outlined in the Acquisition section, comprehensive CT acquisition prior to transcatheter aortic valve procedures should include a multiphase, ECG-gated CTA of the aortic root. Having both systolic and diastolic image reconstructions available is valuable for identification of valve morphology, which in part relies on assessing the opening and closing of commissures.

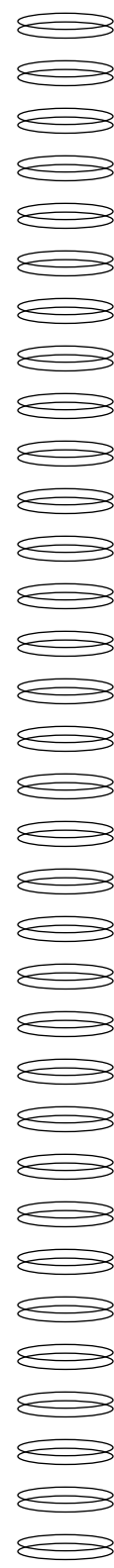
Classification

High-level, tricuspid anatomy with three symmetric cusps and three commissures has to be differentiated from non-tricuspid, ie, bicuspid, anatomy. Bicuspid anatomy is commonly described using the Sievers classification, which differentiates the presence and number of raphe (FIGURE 30):

- Sievers Type 0: Two symmetric cusps, no raphe.
- Sievers Type 1: Two of three cusps conjoined by a raphe.
- Sievers Type 2: Three cusps conjoined by two raphe, one opening commissure (also referred to as unicuspid).

Raphe. In general, raphe refers to a tissue ridge, where two anatomical structures are fused. In bicuspid valves, raphe refers to the tissue ridge between the two conjoined cusps. Anatomically, the raphe is lower than the commissures; the raphe does not attain the plane of the attachments/free margin of the commissures. This is the most important anatomical feature to distinguish a raphe from an incomplete opening commissure, which may not open due to degenerative changes.

Acquired/functional bicuspid morphology refers to valves with a tricuspid anatomy with initially complete opening of all commissures, in which degenerative changes led to leaflet restriction preventing a commissure from opening properly, thereby resembling bicuspid anatomy. The terms *functional/acquired bicuspid* or *tri-commissural bicuspid*, however, are poorly defined. The challenge is to distinguish tricuspid valves with incomplete commissural opening from congenital Sievers Type 1 bicuspid valves.



Bicuspid valve classification	Characteristics	Double-oblique transverse MPR	Volume rendered en face view systole	Volume rendered en face view diastole
Sievers Type 0/ bicommissural non-raphe type	<ul style="list-style-type: none"> • Two fairly symmetric cusps and two commissures. • Each cusp has one most basal insertion point; thus, there is a total of two most basal insertion points. 			
Sievers Type 1/ bicommissural raphe type	<ul style="list-style-type: none"> • Two of three cusps are conjoined by a raphe. • Asymmetric cusp sizes with the cusp opposing the raphe (eg, cusp not participating in raphe formation) being larger than in a tricuspid aortic valve. • Raphe does not extend to the level of the STJ, which is the distinguishing characteristic to a non-opening commissure. • Size of raphe and degree of calcification can vary. <p>Upper row: Noncalcified raphe Middle row: Moderately calcified raphe Lower row: Severely calcified raphe</p>	 	 	
Acquired/ functional bicuspid valve (underlying tricuspid anatomy)	<ul style="list-style-type: none"> • Underlying tricuspid anatomy with symmetric sinus of Valsalva • Nonopening commissure due to degenerative changes (here RL commissure) • Nonopening commissure reaches STJ, which is the distinguishing factor compared to a raphe 			

Figure 30. Classification of bicuspid valve and anatomical characteristics, reproduced with permission from JCTT.

Image Interpretation

Comprehensive assessment of valve morphology can be performed using a stepwise approach, which may be helpful in difficult anatomies in particular. Please refer to FIGURE 31 for an example of this stepwise approach.

1. Observation of commissural movement and opening on transverse cine views.
2. Identification of commissures vs. raphe on transverse view.
3. Identification of commissures vs. raphe on longitudinal view.
4. Assessment of sinus of Valsalva for symmetry/asymmetry.

Stepwise Approach to Identification of Valve Anatomy

	Characteristics	Transverse view	Volume rendered en face
Step 1	Initial assessment of valve morphology demonstrating the absence of an opening commissure between the right and left coronary cusps		
	Comment/level	Transverse view	Coronal reference view
Step 2	Free margin of the two opening commissures: Missing commissure, no tissue (yellow arrow, here between RL)		
	Raphe, further toward LVOT: visualizes raphe as tissue rim (yellow arrow, here between RL)		
	Annular plane		

	Comment/level	Transverse view	Longitudinal reference view
Step 3	Opening RN commissure extends up to STJ (yellow arrow) STJ (dotted yellow line)		
	Opening NL commissure extends up to STJ (yellow arrow) STJ (dotted yellow line)		
	RL raphe does not extend to STJ (yellow arrow) STJ (dotted yellow line)		
	Comment	Transverse view	N/A
Step 4	Asymmetry of cusp/sinus size: The intersection of the sinus-to-commissure measurements are located in an eccentric position (off center).		N/A

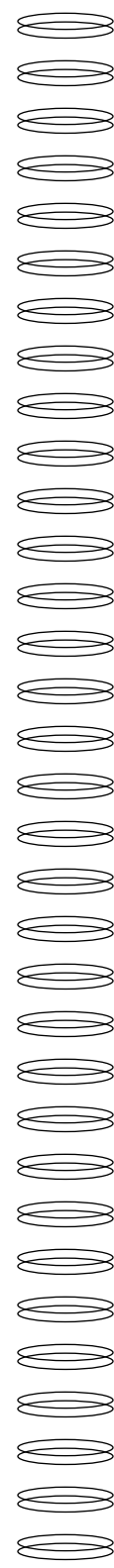
Figure 31. Stepwise approach to identification of valve anatomy and differentiation of bicuspid versus tricuspid anatomy.

Identification of the Annular Plane in Type 0 Bicuspid Aortic Valves

In tricuspid valves and Sievers Type 1 bicuspid valves, three distinct basal cusp insertion points allow for definition of the annular plane. Type 0 bicuspid valves comprise two basal cusp insertion points, which do not lend themselves to reproducible definition of an imaging plane.

The recommended approach is outlined in **FIGURE 32**.

After identifying both basal insertion points and locking them with the crosshairs, the double-oblique transverse plane is adjusted to be perpendicular to the aortic root long axis while, ideally, attaining the smallest cross-sectional area. Over- or under-angulation would result in overestimation of the annular area. The identified plane is also used to determine secondary measurements as well as the required C-arm angulations.



Step and description	Multiplanar reformats
<p>Step 1: Start out with multiplanar images in default axial, sagittal, and coronal orientation; center crosshairs onto the aortic valve.</p>	
<p>Step 2: Align the crosshairs in the sagittal and coronal views with the long axis of the aortic root; the resulting double-oblique transverse view will depict the aortic valve en face.</p>	
<p>Step 3: Move the double-oblique transverse plane up and down to identify the lowest insertion point of the more anterior/lateral cusp. Position the center of the crosshairs exactly at the most basal insertion point (white arrowhead).</p>	
<p>Step 4: Rotate the crosshairs counterclockwise without moving up and down while maintaining its center position so that the formerly coronal view (here red crosshair) transects the lowest insertion point of the medial/posterior cusp (white arrowhead).</p>	

Step and description	Multiplanar reformats
<p>Step 5: The formerly coronal, now double-oblique view will show the lowest insertion points of both cusps (white arrowheads). In this view, rotate the crosshair (here orange) indicating the double-oblique transverse view to transect exactly through the most basal insertion point of the medial/posterior cusp. Once this is achieved, the transverse double-oblique plane will contain the most basal cusp insertion points of both cusps.</p>	
<p>Step 6: Move the center of the crosshairs to the center of the lumen (yellow arrow) without changing the orientation and position of the formerly coronal, now double-oblique view (red crosshair). This is best done by scrolling through the formerly sagittal, now double-oblique view.</p>	
<p>Step 7: In the formerly sagittal, now double-oblique view, rotate the crosshair of the double-oblique transverse plane (here orange) while maintaining alignment with the most basal insertion points (arrowheads) until the smallest cross-sectional area is achieved on the double-oblique transverse plane.</p> <p>CAVEAT: Over- and under-angulation result in overestimation of the cross-sectional area (dashed lines).</p>	

Figure 32. Identification of annular plane in Type 0 bicuspid valves.

Identification of Annular Plane in Type 1 Bicuspid Aortic Valves

Type 1 bicuspid valves, by definition, have three basal hinge points. Utilize these three basal hinge points for identification of the basal plane as routinely done for a tricuspid valve, as outlined on pages 26 and 27.

Transfemoral Access Analysis

The aorta and iliofemoral vasculature should be evaluated using the acquired non-gated CTA data. The aorta can usually be evaluated using axial images and does not necessarily require advanced segmentation. The iliofemoral vasculature should be evaluated using a combination of axial images as well as various post-processing techniques.

Aorta

The thoracic and abdominal aorta should be assessed for the presence of

- Tortuosity, kinking, aneurysm, and in particular partially thrombosed aneurysm
- Noncalcified, exophytic plaque (**FIGURE 33**)

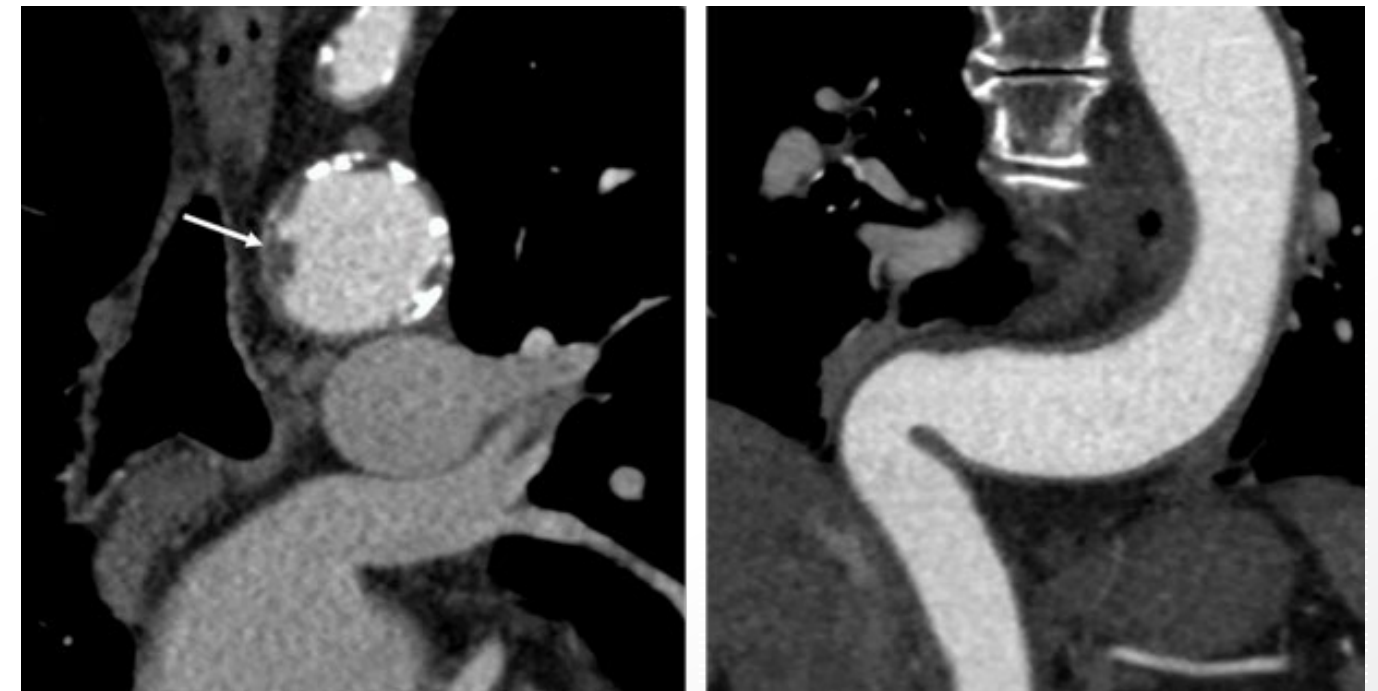


Figure 33. Left: Coronal view demonstrating atherosclerotic changes in the aortic arch, including noncalcified plaque (white arrow). Right: Marked 90-degree kinking of the descending aorta.

Iliofemoral Vasculature

The iliofemoral arteries should be assessed for:

- Vessel diameters
- Vascular calcification
- Tortuosity
- Potential pathology, such as dissections

A comprehensive analysis includes:

- Review of the vasculature on axial images
- Multiplanar reformats (MPRs) or centerline-based curved planar reformats (CPRs)
- Volume-rendered images (VRIs)

Vascular segmentation. Vascular dimensions should be assessed perpendicular to the long axis of the vessel in order to identify the minimal vessel diameter of each iliofemoral vascular axis. On true axial images, only the common femoral arteries are oriented in a perpendicular fashion to the imaging plane while common and external iliac arteries are oriented in an oblique fashion. Thus, true axial source images do not allow for more than a preliminary assessment in regard to iliac artery dimensions.

Dimensions can be assessed using:

- Multiplanar reformats (MPRs), with manual alignment perpendicular to the vessel's long axis at particular locations of interest (**FIGURE 34**). Multiplanar reformats can be cumbersome to less experienced users but allow for precise alignment with the orientation of each vessel segment of interest.
- Curved planar reformats (CPR) when using dedicated post-processing platforms that allow for semi-automated or automated creation of centerlines along the iliofemoral vasculature (**FIGURE 35**). Centerlines allow creation of cross-sectional en face images of the vessel lumen perpendicular to the centerline itself. However, given the semi-automated/automated component of this technique, manual verification of the centerline position is mandatory to ensure accurate vessel tracking and appropriate intraluminal location, in particular, in the setting of calcifications. If the centerline is inappropriately placed, resulting measurements may overestimate vessel dimensions.

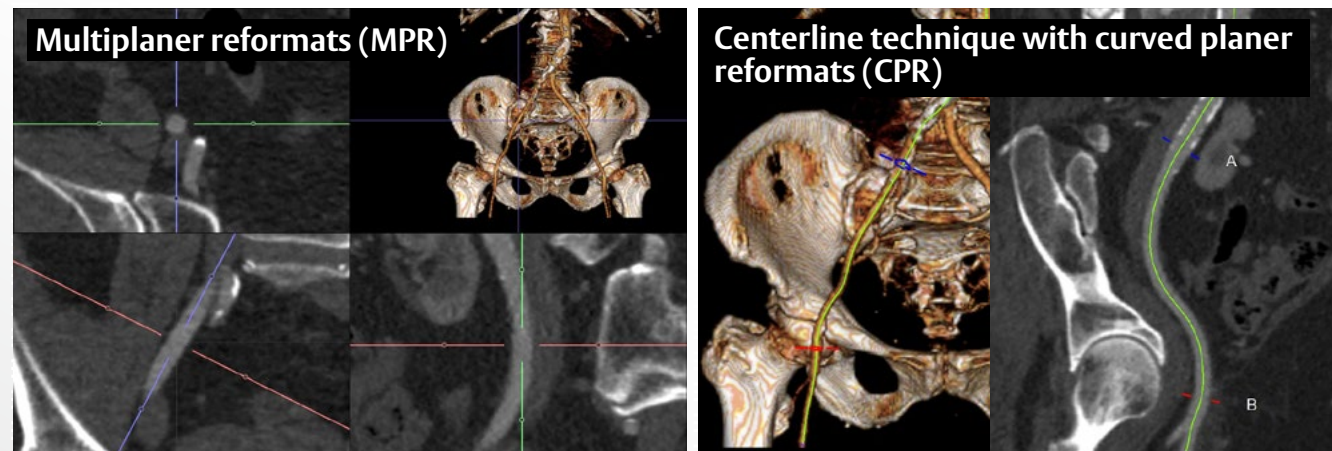


Figure 34. Assessment of vascular dimensions with either multiplanar reformats (MPRs), which are aligned with the vessel long axis to produce a perpendicular cross-sectional view (left), or curved planar reformats (CPRs) using a centerline technique.

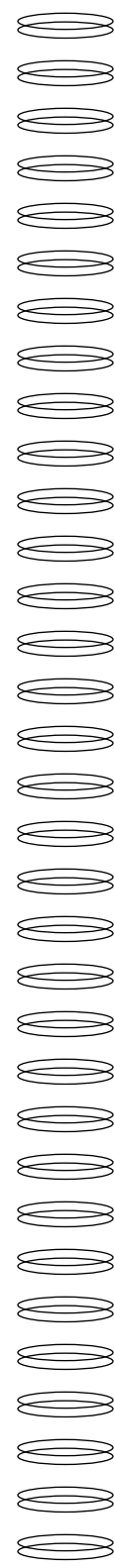


Figure 35. CPRs of the right iliofemoral vasculature with perpendicular short axis views at the level of the common iliac artery and common femoral artery.

Measurements. Quantitative assessment of vessel diameters can be performed by:

- Manual caliper measurements
- Automated contouring

Manual caliper tools provide the most control of the orientation, as well as extent of the measurement (FIGURE 36). The measurement should be taken wall-to-wall in a centered fashion. Automated contouring

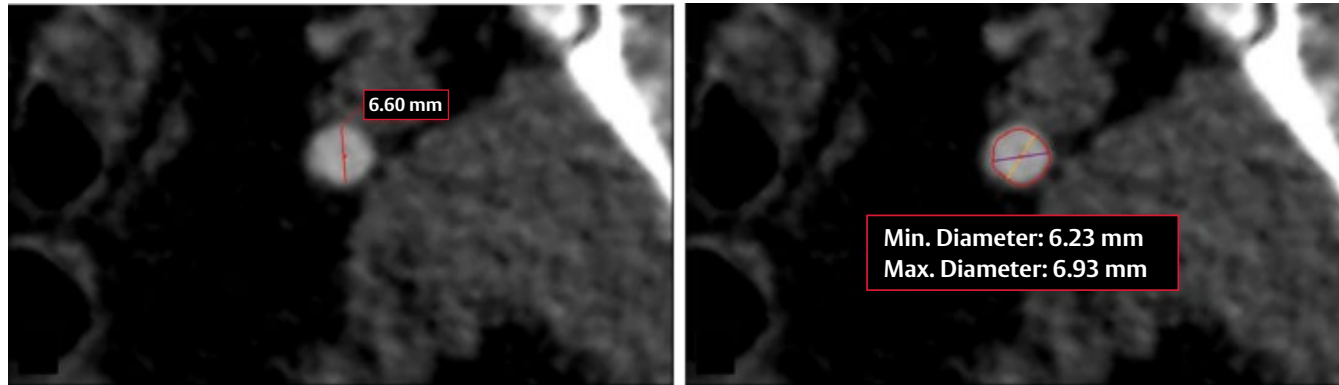


Figure 36. Short axis/en face images of an external iliac artery. The left image demonstrates a manual caliper measurement; the right image illustrates an automated segmentation with presentation of minimum and maximum diameters.

Vascular Calcification

Vascular calcification can be assessed on axial views, CPRs with short axis views and VRTs. Calcifications can, in general, be described and graded with increasing severity in regard to both distribution and configuration (FIGURE 37).

Distribution:

- Spotty
- Confluent, coalescing

Configuration:

- Eccentric, nonprotruding
- Eccentric, protruding
- Horseshoe
- Circumferential

tools commonly detect the vessel wall based on vessel attenuation/CT density with subsequent presentation of maximum and minimum dimensions (FIGURE 36). The quality of these presented dimensions depends heavily on the vessel wall segmentation and routinely requires manual adjustment.

The required vessel diameters depend on the intended device to be used. Please refer to device specific IFUs.

While a large amount of spotty or confluent calcifications can add to friction when introducing the delivery sheath in borderline-sized iliac arteries, the presence of horseshoe and circumferential calcifications may impair necessary vessel expansion when the valve is passed through the sheet.

When reviewing the CTA images, appropriate window settings should be applied to allow to distinguish between contrast-enhanced blood-pool and calcification. Windowing is the process in which the CT image gray-scale component of an image is adjusted, thereby changing the appearance of the picture to highlight particular structures (FIGURE 38). The brightness of the image is adjusted via the window level (L). The contrast is adjusted via the window width (W).

Calcifications are known to appear more prominent on CT imaging than they are in reality; this is referred to as calcium blooming. The window level has an impact on the appearance of calcium and the extent of calcium blooming, with wider windows at a higher level (eg,

bone window) tremendously reducing the blooming (FIGURE 38). For calcified segments, a wider window should be employed in order to avoid underestimation of the true vascular lumen (FIGURE 39).

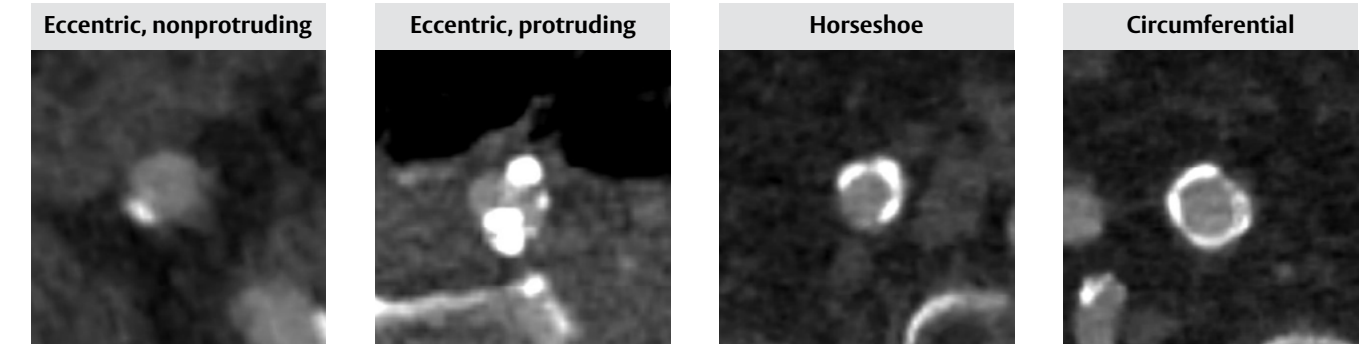


Figure 37. Examples of increasing severity of calcium in regard to its configuration.

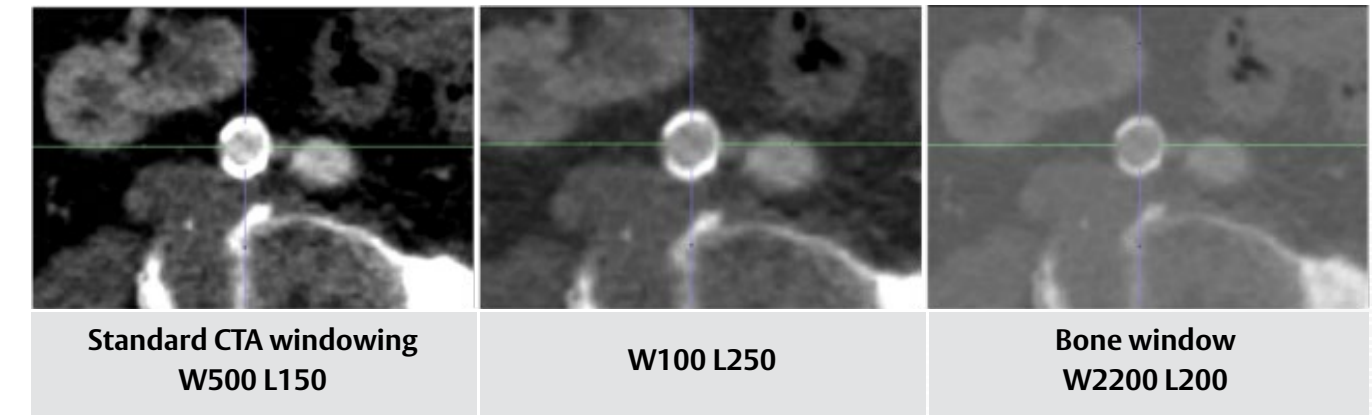


Figure 38. Demonstration of the impact of window leveling onto the appearance of vascular calcification in the setting of a near-circumferential calcification of the right common iliac artery. A wider window setting decreases the amount of calcium blooming.

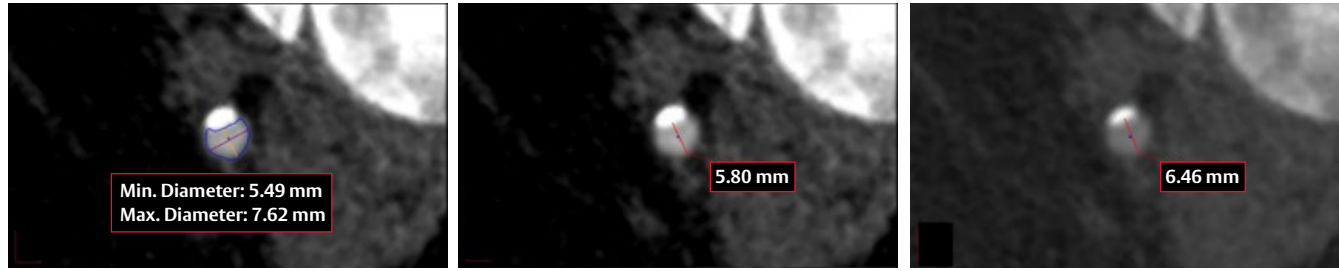


Figure 39. Impact of measurement technique and window setting onto the assessed diameter value. Left and middle images are displayed in a standard CTA window setting, with the left image showing an automated segmentation that suffers from complete exclusion of the blooming calcium, and a manual measurement in the middle image accounting for the blooming by slightly extending into it. The right image is displayed in a wide window setting to reduce the calcium blooming, potentially avoiding underestimation of the diameter.

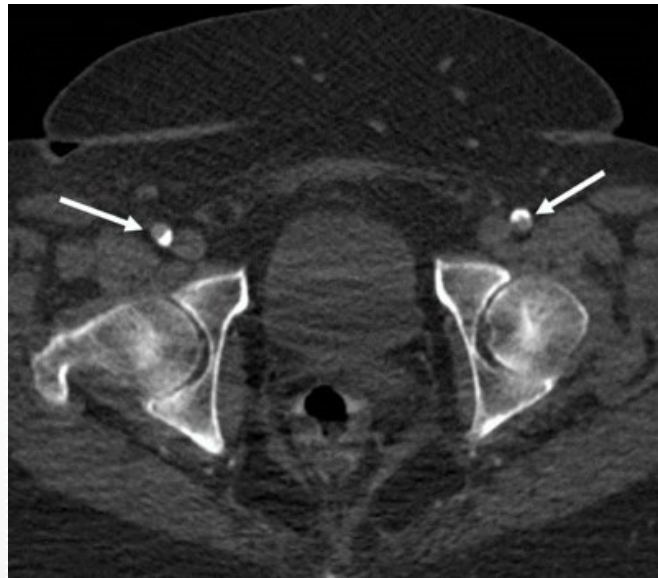


Figure 40. Axial image at the level of the common femoral arteries (white arrows). Calcifications are located posteriorly on the right and anteriorly on the left. In addition, note the adipose habitus that may impact vascular puncture.

Access site. In particular, the location and degree of calcifications at the level of the puncture site at the common femoral artery should be assessed. Anteriorly located calcification may interfere with suture systems commonly used for a totally percutaneous, transfemoral approach (FIGURE 40). Relevant findings should be reported, ideally with detailed location in relation to fluoroscopically identifiable anatomical landmarks, such as the level of the femoral head (eg, lower third) (FIGURE 41). The anatomy should also be reviewed for presence of a high femoral artery bifurcation.

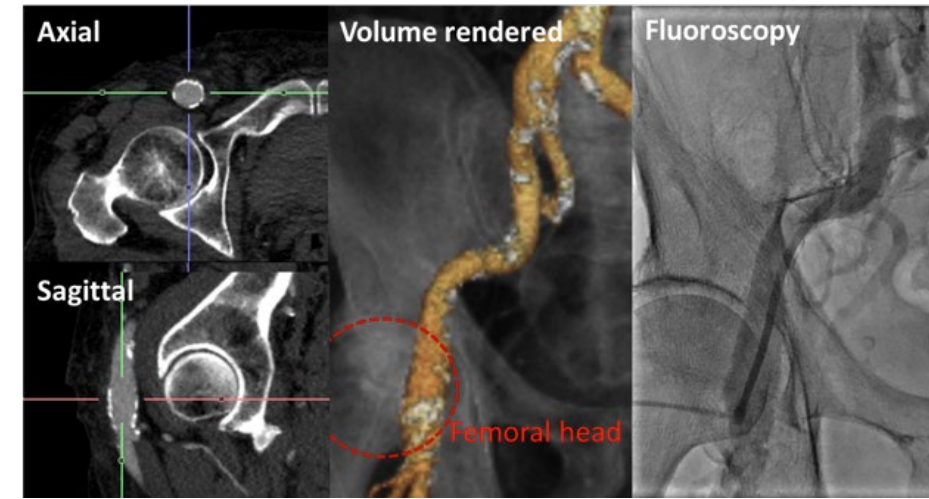


Figure 41. CT images should be assessed for anatomy and presence of calcifications at the access site, referenced to the femoral head, which acts as a landmark on both CT and fluoroscopy. Here, anterior located calcification below the center of the femoral head that was avoided in the subsequent arterial puncture.

Tortuosity

Vascular tortuosity can be best assessed on volume-rendered images given the 3D nature of this technique. Importantly, assessment should not be confined to anterior-posterior projection only but should also include oblique projections, as anterior-

posterior projections often may not provide the full extent of tortuosity (FIGURE 42). The quantification of tortuosity itself is not standardized. For documentation, AP and oblique views of the iliac vasculature should be obtained.

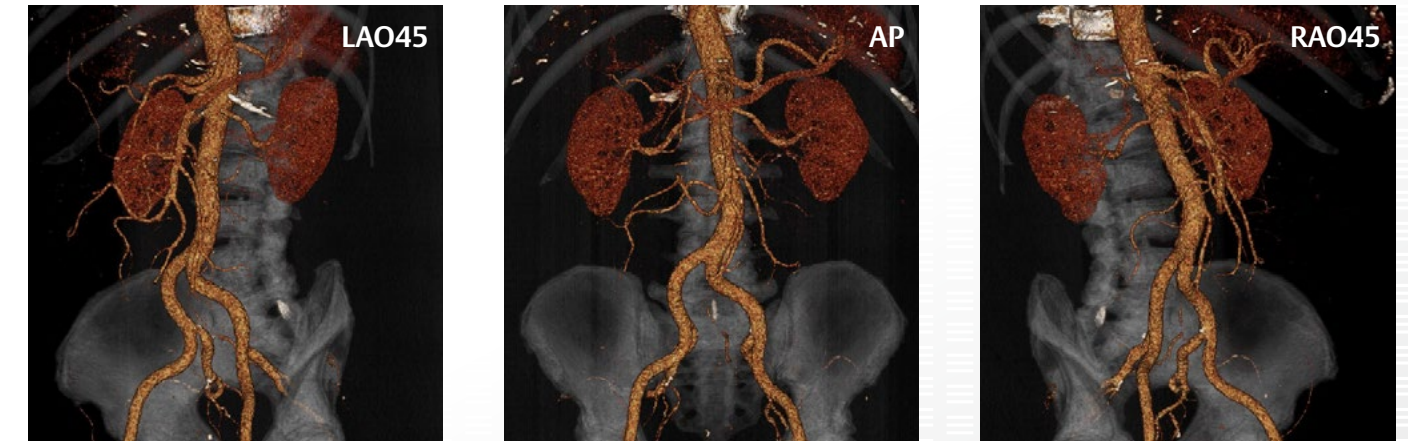


Figure 42. Volume-rendered images in LAO (left), AP (middle), and RAO (right) projection for assessment of iliofemoral tortuosity.

Subclavian and Axillary Access Analysis

The subclavian and axillary artery can be used as an alternative access if the patient's anatomy is not suitable for transfemoral access.

In general, the patient's left side is preferred for subclavian and axillary access due to a more pronounced angulation/double angulation of the path of the right subclavian artery.

If subclavian or axillary access is an available alternative at the treating institution, the following recommendation for CT data acquisition should be considered:

- The volume of the non-gated CTA of the chest, abdomen, and pelvis should be extended cephalad to include the upper thoracic aperture and clavicles to ensure sufficient coverage of the potential access route.
- Contrast administration should be performed via the right upper extremity to avoid streak artifacts on the left side, which could potentially limit the access evaluation.
- Acquisition parameters and technique can otherwise remain unchanged.
- Note: The arms should remain elevated to ensure adequate image quality at the level of the aortic root. This may distort the anatomy at the level of the axillary artery; take this into consideration when performing access assessment.

Image Analysis

Vessel Depth

- The depth of the subclavian and axillary artery in regard to the anterior body surface is particularly important for a percutaneous transaxillary

approach, a larger depth (eg, >6 cm) adds to the complexity of the procedure with modification of the access point to optimize the sheath entry point angle.

- Measurement techniques are illustrated in **FIGURE 43**. Arm position during CT may alter the assessed value.

Vessel Dimensions

- Assessment of vessel diameter should include the following locations, using either multiplanar reformats or curved planar reformats (centerline):
 - ~ Takeoff of subclavian or innominate artery from the arch
 - ~ Level of origin of the vertebral artery
 - ~ Underneath the clavicle
 - ~ Level of the minor pectoralis muscle (location of the incision for transaxillary approach)
 - ~ Any other point of interest, such as focal stenosis
- Segmentation and measurement techniques are similar to the techniques applied for transfemoral access evaluation. Centerline assessment is illustrated in **FIGURE 44**.

Calcification

- The access route should be assessed for presence, distribution, and severity of calcification.
- In particular, the origin at the aortic arch should be assessed for the presence of calcium, as calcification in this location may increase the risk of vascular injury. An example is shown in **FIGURE 45**.

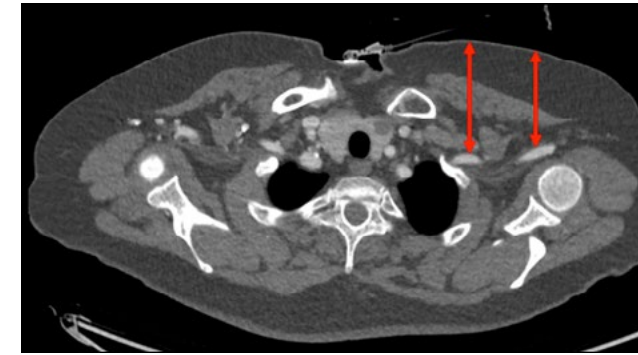


Figure 43. Assessment of the depth of the subclavian and axillary artery to the anterior body surface. Measurements are taken in a straight anterior-posterior orientation from the body surface to the anterior aspect of the artery using standard axial source images.

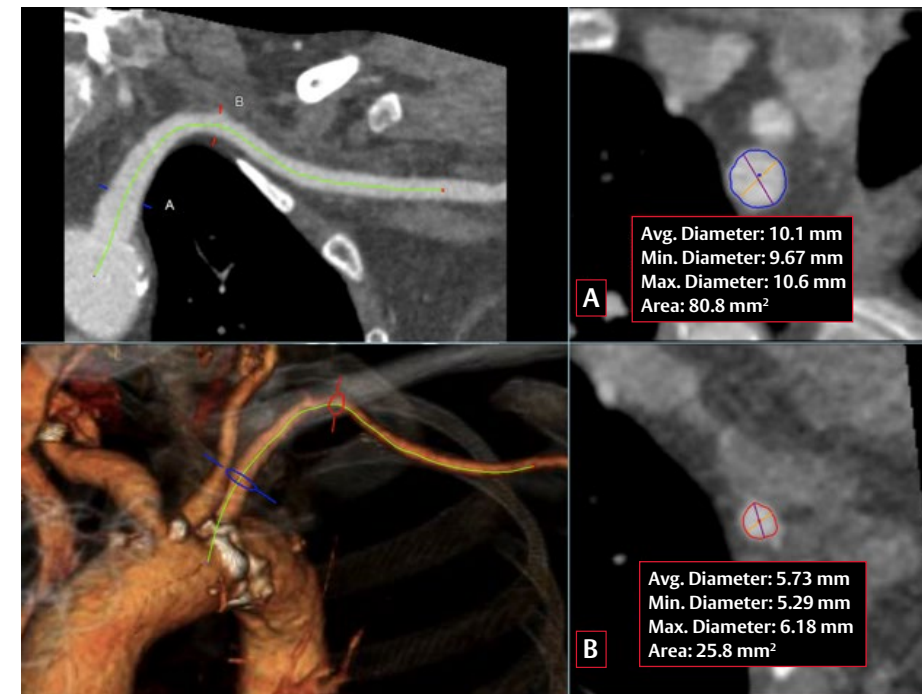


Figure 44. Assessment of left subclavian and axillary artery dimensions using centerline technique.

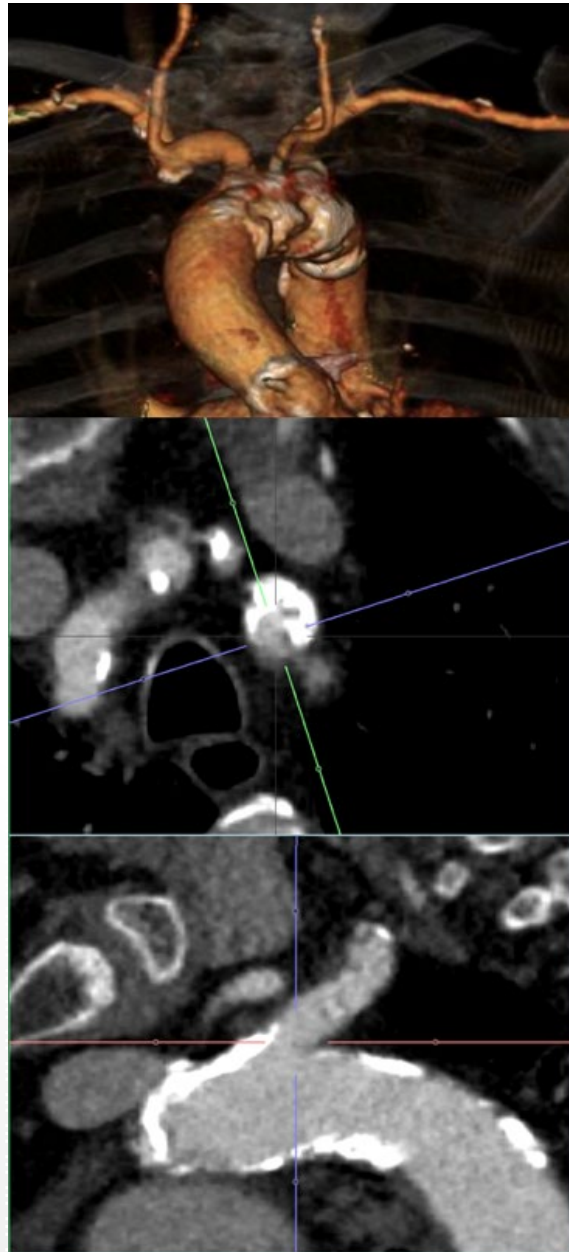


Figure 45. Example of severe bulky calcification at the origin of the left subclavian artery.

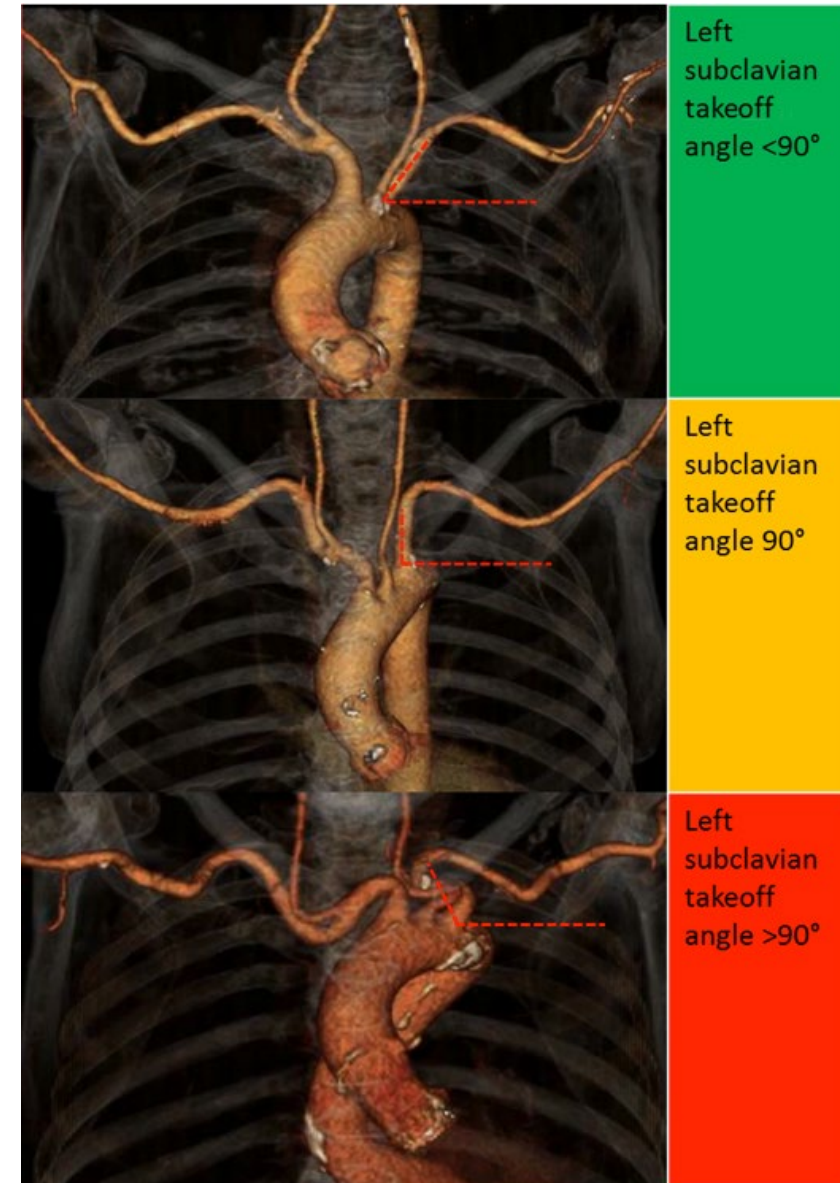
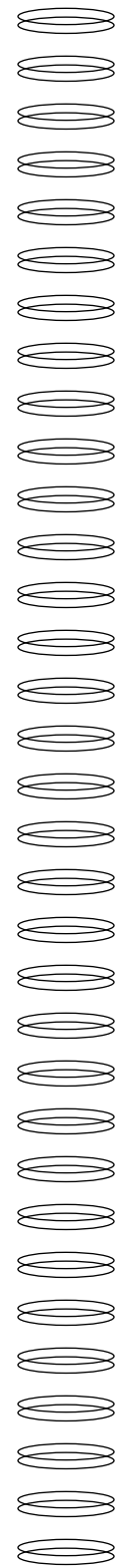


Figure 46. Angulation of the origin of the left subclavian artery displayed using volume-rendered technique in an AP perspective. Measurements are taken with the vertex of the angle at the origin of the subclavian artery, and one side adjusted along the subclavian artery to the origin of the vertebral artery, and the other side representing the horizontal plane. A takeoff angle of $< 90^\circ$ is preferred.

Additional Assessment for Transaortic or Transapical Approach



Figure 47. Assessment of ascending aorta orientation.

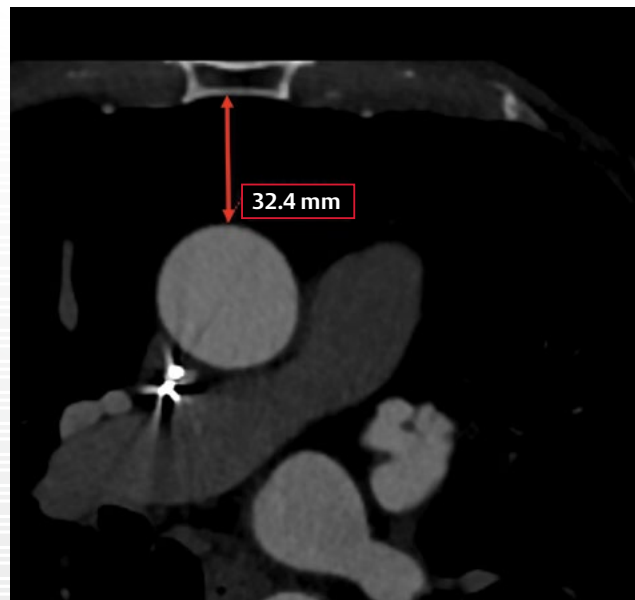


Figure 48. Assessment of the aorta to sternum distance.

Transaortic Approach

Assessment for transaortic approach includes:

- Ascending aortic length
- Aortic annular angulation
- Distance between aorta and sternum
- Other considerations

Ascending Aortic Length

Step 1

Do NOT change the angulation or level of the annular plane (transverse double-oblique image).

Step 2

Measure the distance from the annular plane to the transection point of the crosshairs and the ascending aortic wall on either coronal oblique or sagittal oblique view (both views result in the same measurement) (FIGURE 49).

Aortic Annular Angulation

Step 1

Do NOT change the angulation or level of the annular plane (transverse double-oblique image).

Step 2

Assess the angulation of the annular plane in regard to the horizontal axis (FIGURE 47).

Ascending Aortic Length

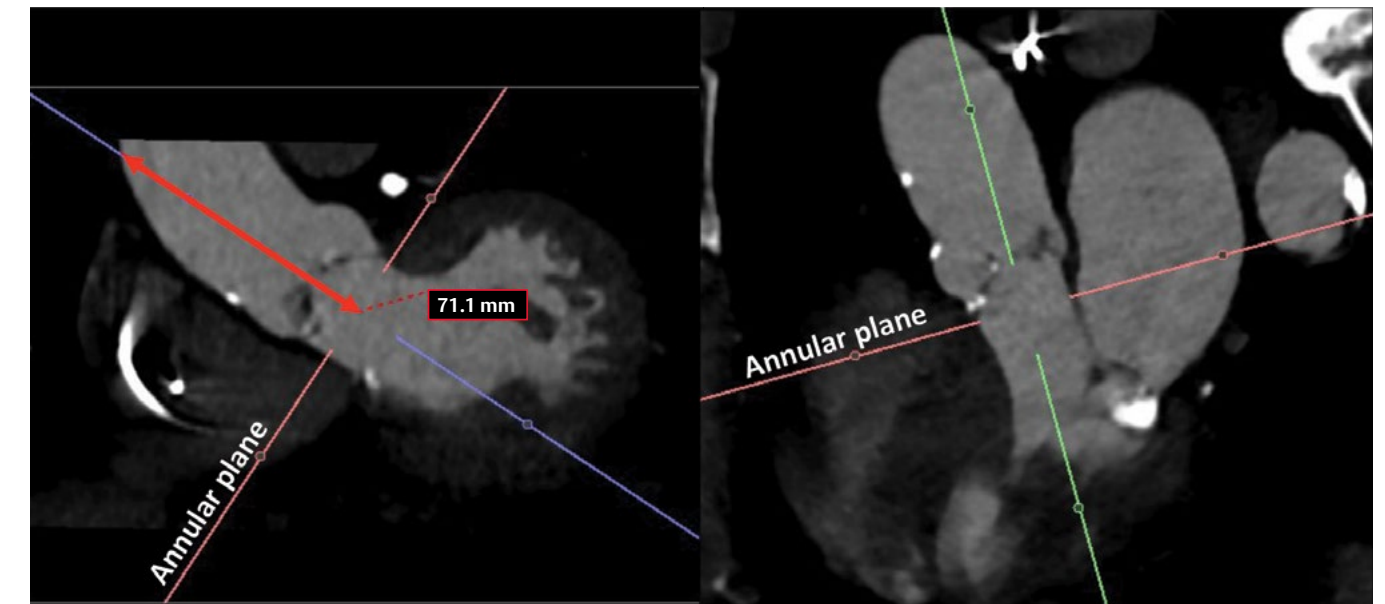


Figure 49. Assessment of ascending aortic length.

This measurement is needed for evaluating the feasibility of transaortic access.

Distance Between Aorta and Sternum

Measure the distance between the anterior aspect of the ascending aorta and the posterior aspect of the sternum on a true axial image (FIGURE 48). If the axial CT images demonstrate that the aorta is central, posterior to the sternum, or left of the sternum, an upper mini-sternotomy is recommended.

Other Considerations

- If the axial CT views demonstrate that the aorta is to the right of the sternum and/or horizontal (angle $>40^\circ$ - $>45^\circ$), a mini-thoracotomy is suggested, unless other specific anatomical or clinical contraindications exist. If the horizontal aortic annular angulation is $>75^\circ$ (pronounced

horizontal), a transapical approach may be preferred.

- 3D volume-rendered and multiplanar reconstructions are recommended for assessing the ideal puncture site and incision.
- Refer to the IFU for approach-specific contraindications.

Transapical Approach

- Assess location of apex in relationship to the intercostal space and chest wall.
- Note chest wall thickness.
- Refer to the IFU for approach-specific contraindications.

Assessment for Transseptal Access

The following section describes the image analysis for assessment prior to transseptal access for, eg, mitral Valve-in-Valve procedures.

The following items should be assessed:

- Height of the fossa ovalis (minimal and maximum height (**FIGURE 50**))
- Left atrial dimensions (left atrial height, **FIGURE 50**)
- Septal thickness; abnormal findings, such as lipomatous hypertrophy, patent foramen ovale, or atrial septal defect (**FIGURE 51**)

Assessment can be performed using either standard multiplanar reformats (MPRs) or advanced post-processing workflows. Measurements for fossa ovalis height and left atrial height are taken perpendicular to the plane of the surgical mitral prosthesis.

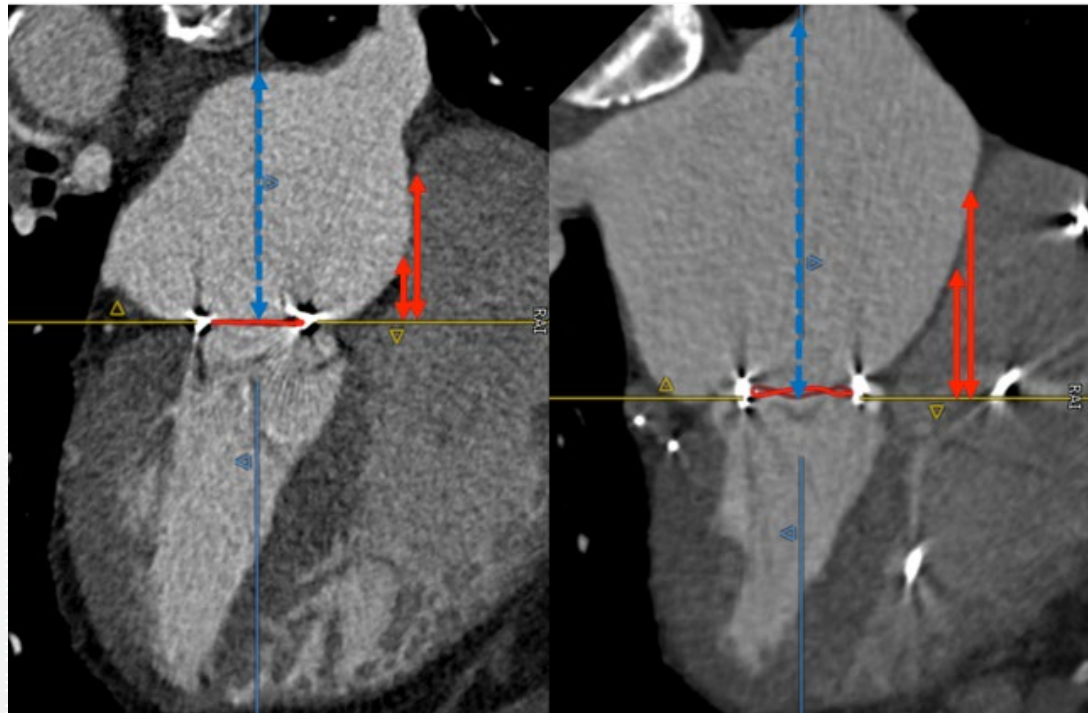


Figure 50. Two examples of left atrial height (blue arrow) and fossa ovalis height assessment (red arrows). Measurements are taken perpendicular to the orientation of the basal sewing ring of the surgical mitral valve prosthesis. For fossa ovalis height, measurements are taken to the lower and upper margin of the fossa ovalis (minimum and maximum height).

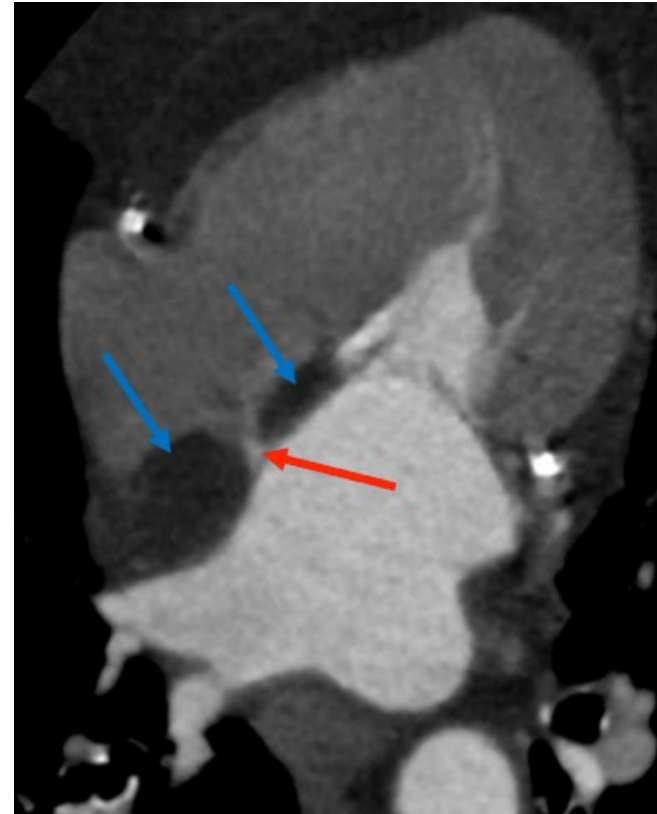
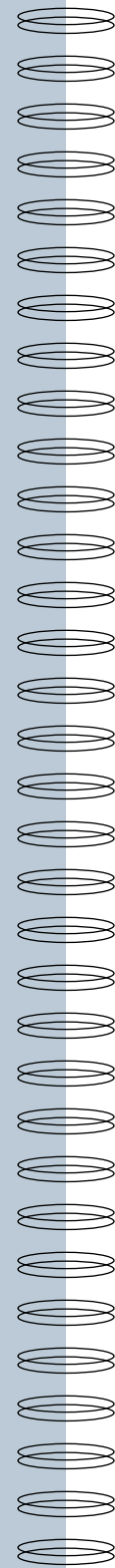


Figure 51. Example of lipomatous hypertrophy of the interatrial septum. Blue arrows illustrate the lipomatous hypertrophy, and the red arrow indicates the fossa ovalis.



Troubleshooting

Accurate assessment of the aortic annulus and aortic root requires good image quality characterized by sufficient contrast enhancement, sharp anatomical contours, and the absence of artifacts. Inaccurate assessment may be attributed to:

- Improper measurement technique
- Insufficient image quality

Importantly, critical measurements, such as annular measurements, should be documented by means of screenshots (eg, secondary captures), which are ideally archived in the PACS (Picture Archiving and Communication System).

Screenshots should not include only the view in which the measurement was taken but also the adjunct views, such as the coronal and sagittal double-oblique views, in case of an annular measurement on the double-oblique transverse view. These comprehensive screenshots provide the following valuable information:

- Positioning of the measurement plane
- Overall image quality
- Artifacts, which may be subtle or obscured on the measurement plane but more evident on others

Correct Orientation of the Annular Plane

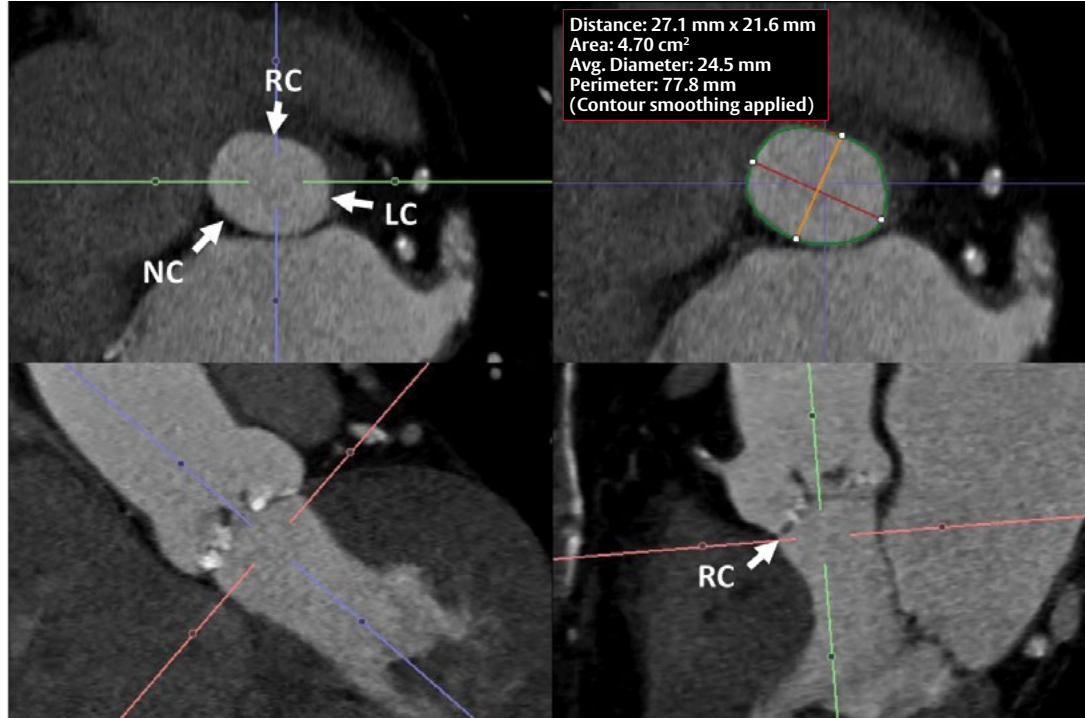


Figure 52. Appropriate annular plane segmentation and planimetry.

As discussed earlier, the annular plane transects through the most basal hinge points of all three cusps. Commonly, the center of the crosshairs remains in the center of the annular lumen when obtaining the screenshot (**FIGURE 52**).

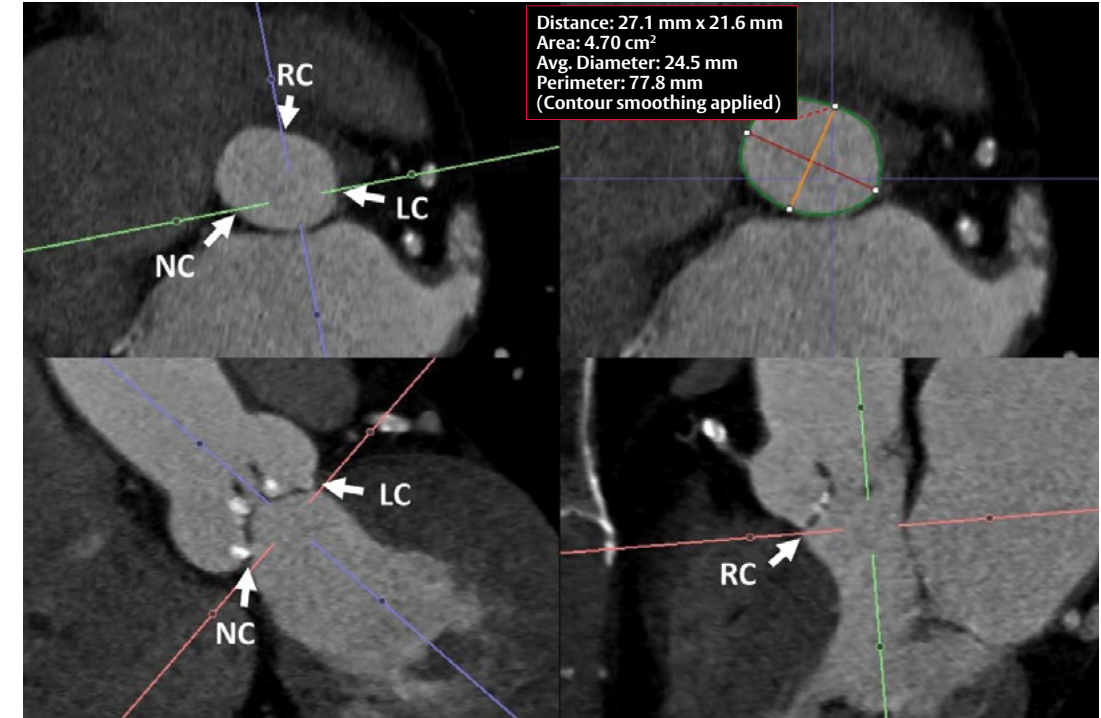


Figure 53. Appropriate annular plane segmentation and planimetry with crosshairs oriented to show all three hinge points. RC, right coronary cusp; LC, left coronary cusp; NC, non-coronary cusp. Same patient as shown in Figure 37.

Crosshairs typically have a color-coding for users to recognize the view/plane that they are representing, with the colors used being software-manufacturer-specific. In the examples shown in Figure 37, the red lines in the oblique coronal and sagittal images indicate the location of the double-oblique transverse image. As the crosshairs actually transect the annular contour four times at 90° intervals, not all of the three

hinge points are depicted on the coronal and sagittal oblique views at the same time if the crosshairs remain centered in the annular lumen.

Alternatively, the crosshairs can be oriented to transect all three basal hinge points by eccentric orientation of the crosshair center (**FIGURE 53**).

Incorrect Plane – Wrong Orientation

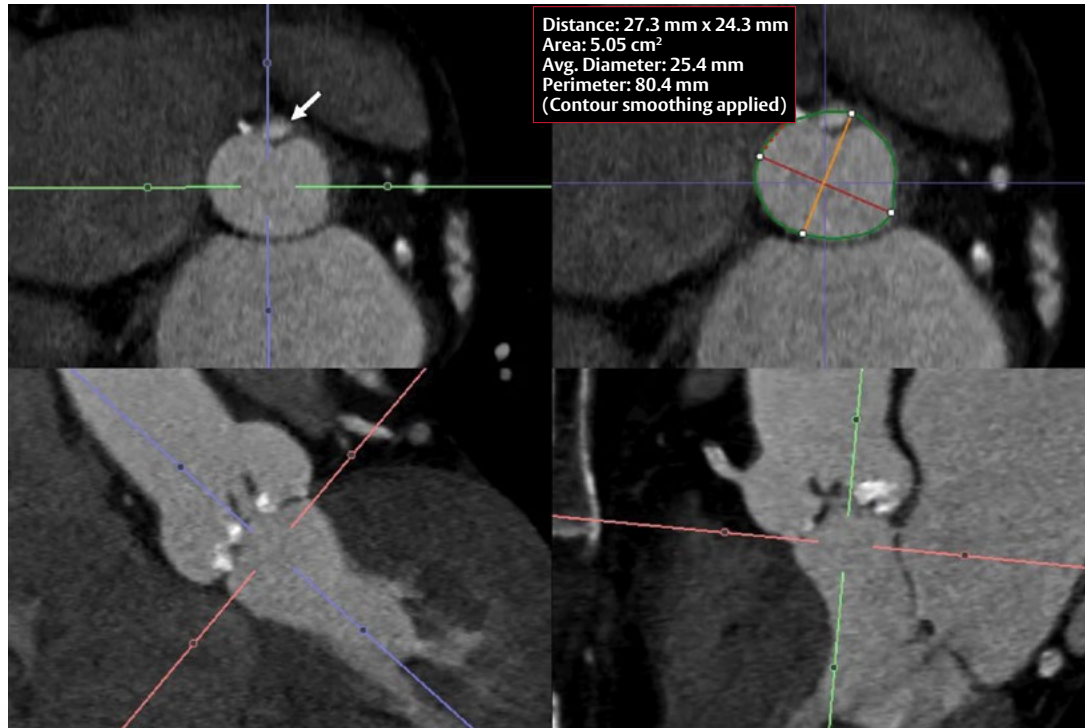


Figure 54. Incorrect plane due to wrong orientation. The plane cuts through the right coronary sinus.

- Incorrect orientation of the annular plane is a common cause of erroneous annular measurements. Frequently, the annular plane transects the basal portion of one sinus as opposed to the most basal hinge point while the two other most basal hinge points are correctly identified.
- In **FIGURE 54**, the red lines in the oblique coronal and sagittal images indicate the location of the double-oblique axial image. Portions of the right coronary cusp can be visualized (white arrow) in the double-oblique transverse view.
- Incorrect angulation commonly results in too-large planimetric measurements.

Incorrect Plane – Wrong Angulation and Too Low

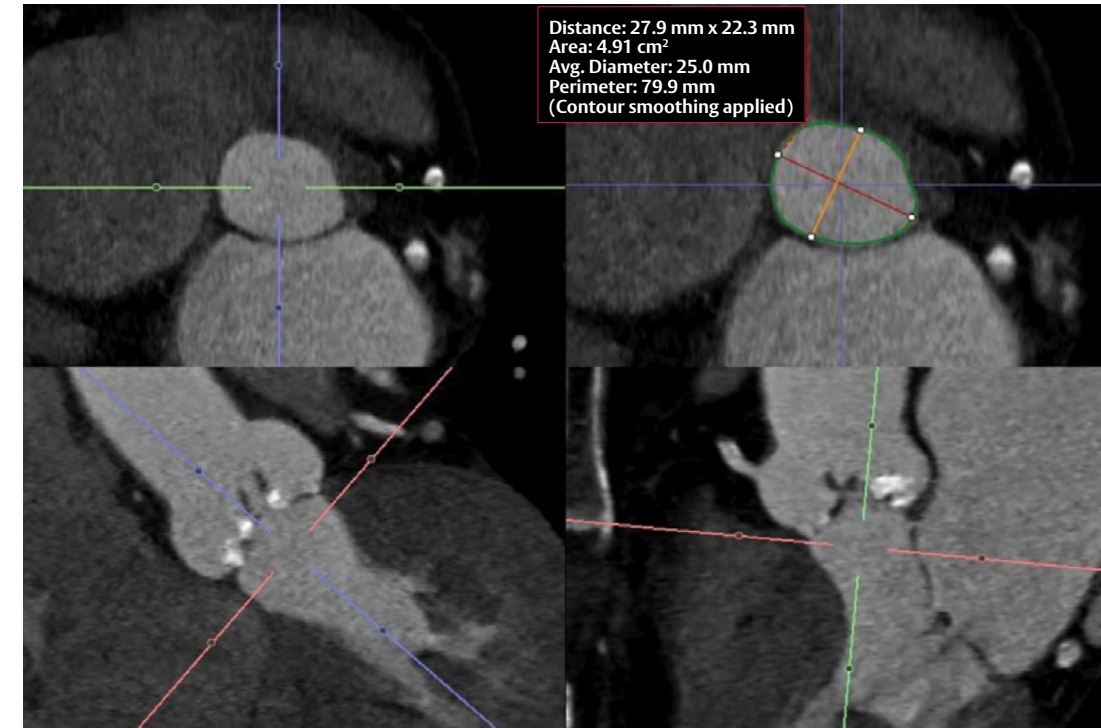


Figure 55. Wrong angulation and too low. Same angulation as in Figure 53.

- In the setting of wrong angulation (**FIGURE 55**), a transverse image without sinus tissue can be generated by relocating the level of the transverse double-oblique plane toward the LVOT. Although the contour on the transverse double-oblique view appears harmonic, it does not resemble the annular plane. As a consequence, planimetric assessment commonly results in too-large measurements.

Incorrect Plane – Too High

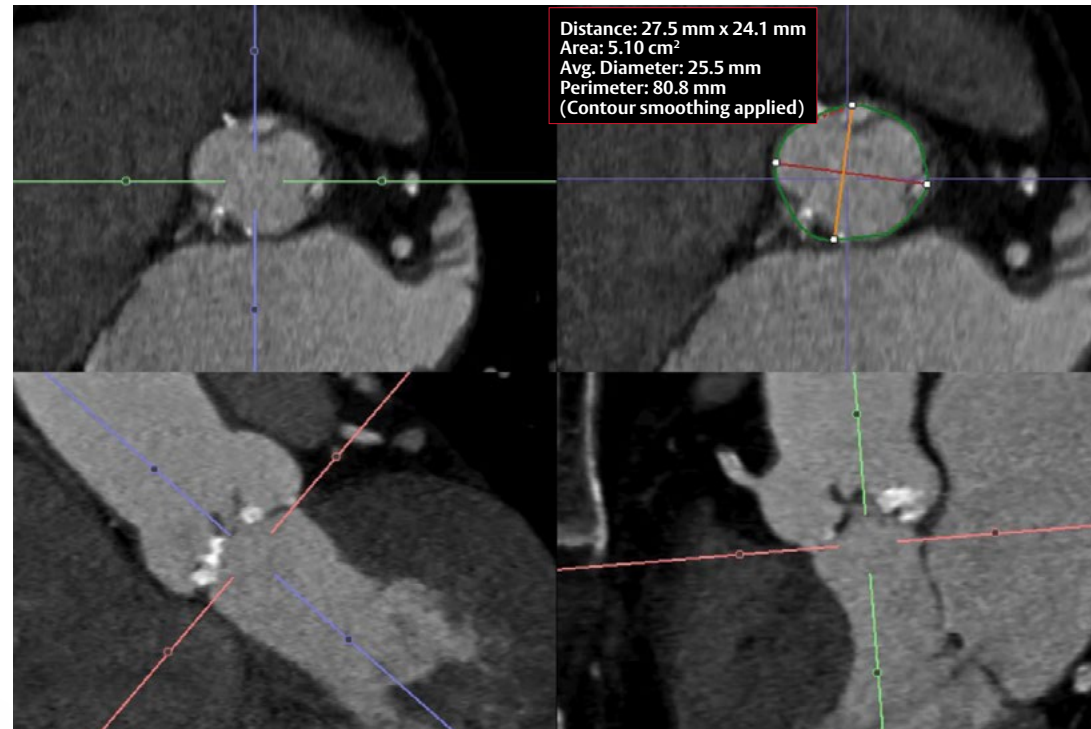


Figure 56. Transverse plane located above the proper annular plane.

- Red lines in the oblique coronal and sagittal images demonstrate the location of the double-oblique axial image. In the double-oblique axial image, all three coronary cusps are visualized, clearly demonstrating that the plane is too high. This commonly results in overestimation of the annular area (FIGURE 56).

Misalignment Artifacts

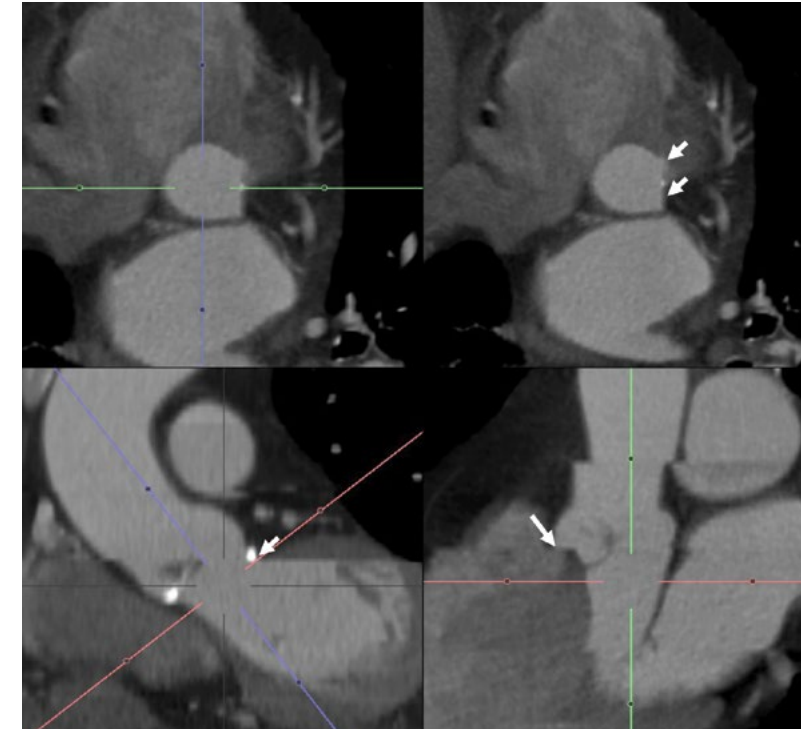


Figure 57. Misalignment artifacts (white arrows) truncating the annular contour.

- Irregular heart rhythms, such as atrial fibrillation, or premature contractions may result in misalignment artifacts due to the variable length of the RR intervals.
- Severe misalignment artifact at the annular level (**white arrows, FIGURE 57**) precludes accurate annular assessment.
- If the image was acquired using retrospective ECG-gating, ECG-editing at the CT scanner console can be useful to reduce the artifact burden.

Double Contours and Blurring

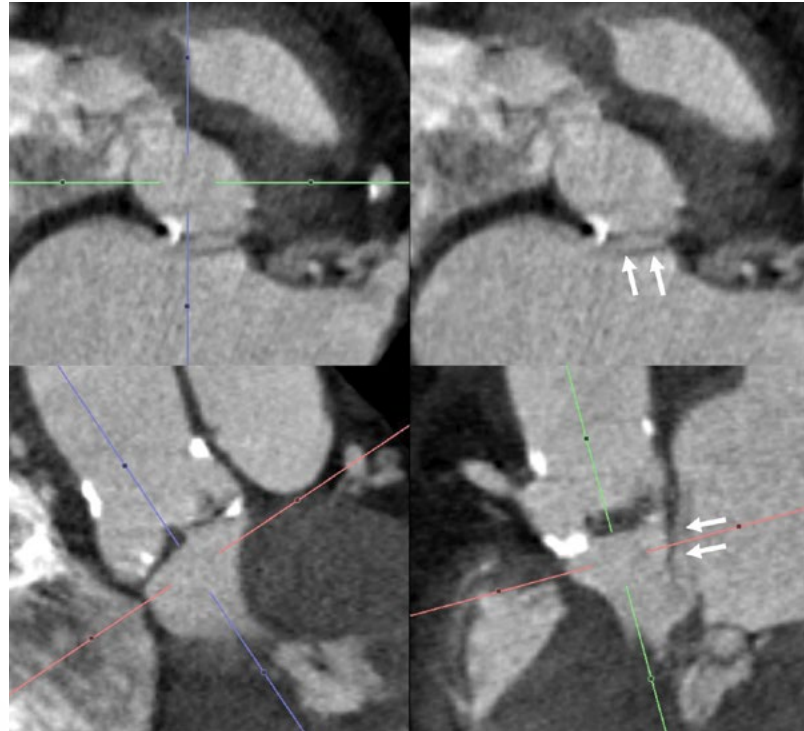


Figure 58. Double contours (white arrows) impairing proper annular assessment.

- Cardiac motion and pulsation in addition to irregular heart rhythms, such as atrial fibrillation or premature contractions may result in double contours and blurring of the annular contour (white arrows, FIGURE 58).
- Severe artifacts or too low contrast opacification (FIGURE 59) preclude accurate annular assessment.

Poor Contrast Enhancement and Image Noise

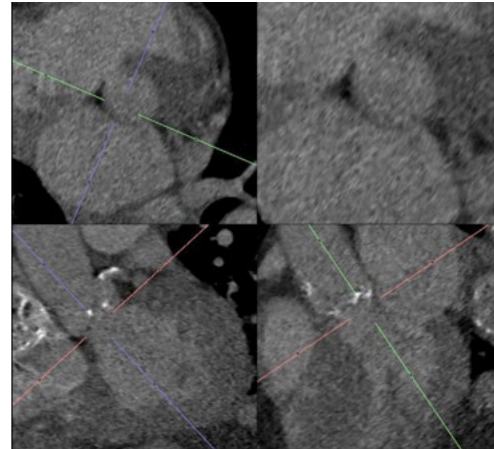


Figure 59. Poor opacification and increased image noise render this data set uninterpretable.

Breathing Artifacts

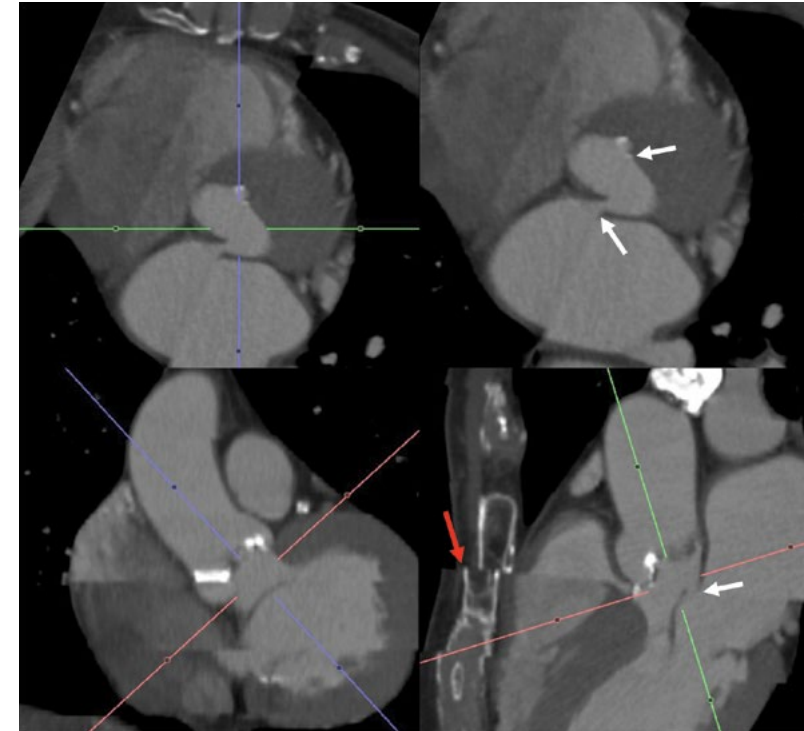


Figure 60. Breathing artifacts at the level of the aortic root (white arrows) and evident as a stair-step also involving the sternum (red arrow).

- Breathing artifacts at the annular level can cause artifacts with a similar appearance as misalignment artifacts (white arrows, FIGURE 60).
- Breathing artifacts always involve the chest wall, commonly appreciated as a stair-step along the body surface or sternum (red arrow, FIGURE 60).
- Breathing artifacts usually preclude accurate annular assessment.

ECG-Editing

- ECG-editing refers to manually correcting synchronization points, as well as selecting/deselecting image data to contribute to image reconstruction.
- The latitude of possibilities depends on the scanner system and the acquisition mode employed.
- Retrospective ECG-gating captures redundant image data that allows for more leeway in regard to image reconstruction and data salvage, in case of artifacts.

	Scanner system with limited z-axis coverage (single- and dual-source systems)				With wholeheart coverage (Aquilion ONE, GE Revolution, CardioGraphe)
	Helical/spiral data acquisition with retrospective ECG-gating	Axial data acquisition with prospective ECG-triggering with padding	Axial data acquisition with prospective ECG-triggering without padding	High-pitch helical data acquisition with prospective ECG-triggering	ECG-gated, one beat, one-slab acquisition with coverage of entire cardiac cycle
Correction of R-peak registration	+	+	+	+	+
Exclusion of image data of an RR interval from image reconstruction	+	-	-	-	N/A

Table 3

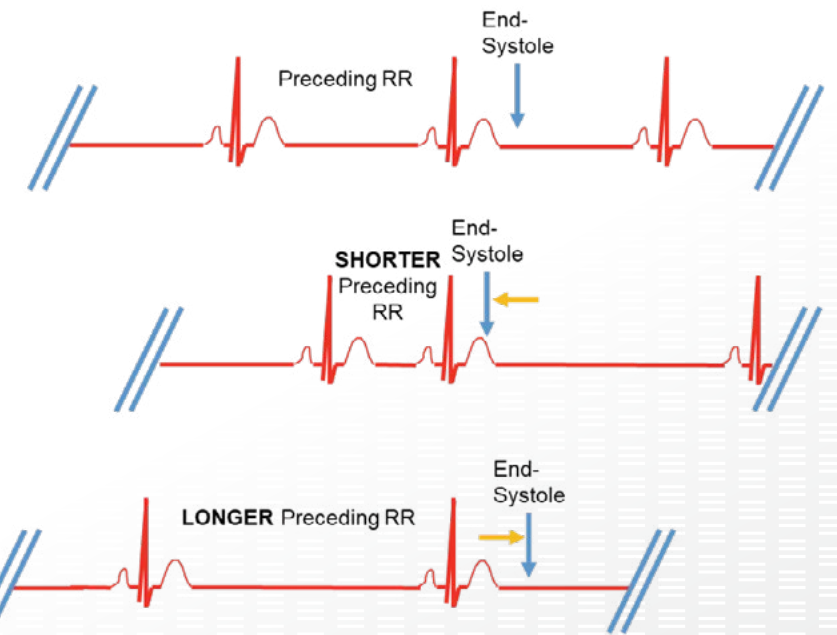
ECG-Synchronization/Correction of R-Peak Registration

- Ensure that the scanner system correctly identified the R-peaks before initiating image reconstruction.
- Artifacts, pronounced T-waves, and pacemaker spikes may be misinterpreted as R-peaks causing mis-synchronization artifacts.
- If not corrected, mis-synchronization leads to
 - ~ Stair-step artifacts when using scanner systems with limited detector coverage
 - ~ Erroneous labeling of reconstruction phases and potentially reconstructing only parts of the cardiac cycle when using volume scanners
- Manually correct the R-peak recognition if necessary.

Exclusion of Image Data From Image Reconstruction (Retrospective ECG-Gating Only)

- Premature contractions result in RR intervals of significantly different lengths, which impact LV filling state (FIGURE 61).
- Differences in LV filling state and alteration of LV ejection time due to differences in the filling state are the substrate of stair-step artifacts.
- Exclusion of CT data from RR intervals affected by premature contractions can resolve stair-step artifacts.
- Best results are commonly achieved for reconstructions focusing on end-systole.
- In order to understand which RR intervals to exclude from image reconstruction, one has to consider the impact of RR-interval length on the occurrence of end-systole within the cardiac cycle:

- ~ Left ventricular ejection time and thus end-systole depend on the extent of diastolic filling and thus the length of the preceding RR interval.
- ~ Left ventricular ejection time is shortened and end-systole occurs earlier in the cardiac cycle (closer to the R-peak), if the preceding RR interval is shortened (less diastolic filling).
- ~ Left ventricular ejection time is lengthened and end-systole occurs later in the cardiac cycle (further away from the R-peak), if the preceding RR-interval length is lengthened.



If the preceding RR interval is shorter, LV filling is reduced and the subsequent LV ejection time is shorter.

If the preceding RR interval is longer, LV filling is increased and the LV ejection time is longer.

Figure 61. Impact of preceding RR-interval length on position of end-systole.

Premature Atrial Contraction

- Premature atrial contractions (PAC) commonly have a similar morphology, as the remainder QRS complexes (usually narrow) (FIGURE 62).
- PACs terminate RR interval early, limiting diastolic filling. The following RR interval is of normal length, but end-systole occurs early due to limited diastolic filling in the preceding RR interval.
- The RR interval beginning with the PAC should be excluded from image reconstruction, when reconstructing absolute (msec) images at end-systole. The RR interval terminated early can contribute to image reconstruction.

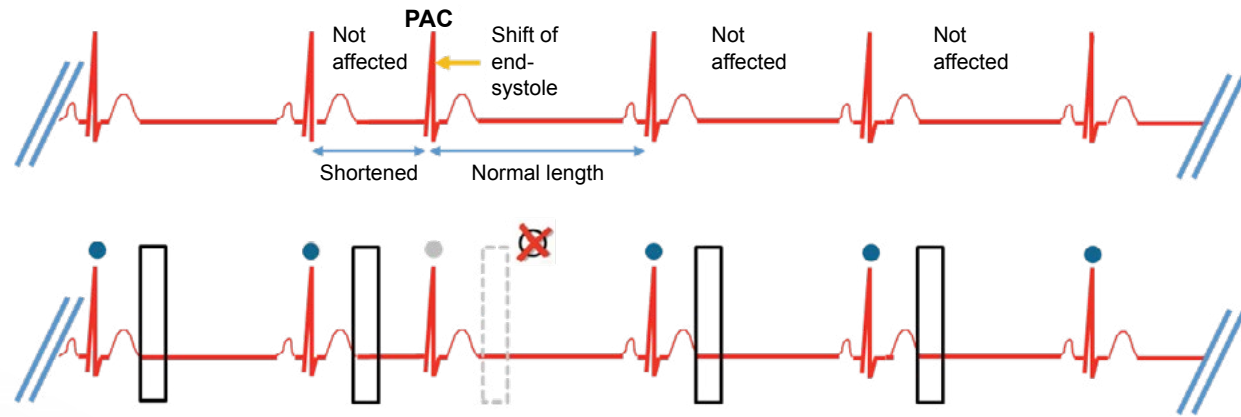


Figure 62. Premature atrial contraction – Absolute (msec) image reconstruction at end-systole.

Premature Ventricular Contraction

- Premature ventricular contractions (PVC) commonly have a wider morphology than the remainder QRS complexes (FIGURE 63).
- PVCs terminate RR interval early, limiting diastolic filling. The following RR interval is lengthened due to the compensatory pause. Within the RR interval beginning with the PVC, end-systole occurs early due to limited diastolic filling in the preceding RR interval. Within the subsequent RR interval, end-systole occurs later due to increased diastolic filling during the compensatory pause.
- The RR interval beginning with the PVC, as well as the subsequent RR interval, should be excluded from image reconstruction; when reconstructing absolute (msec) images at end-systole. The RR interval when terminated early can contribute to image reconstruction.

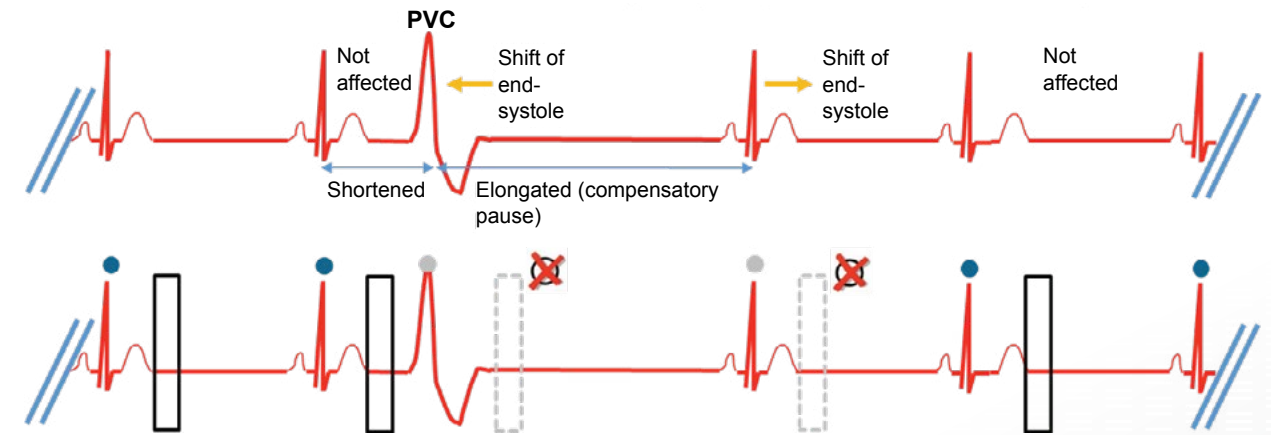
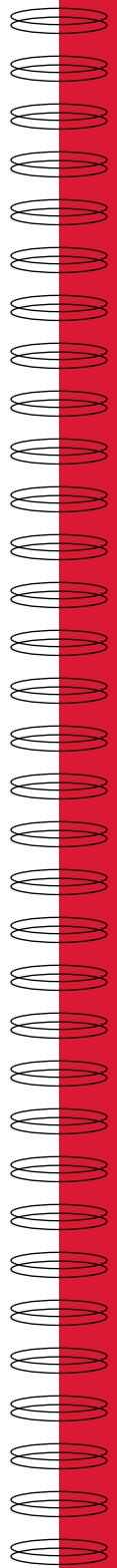


Figure 63. Premature ventricular contraction – Absolute (msec) image reconstruction at end-systole.



Bibliography

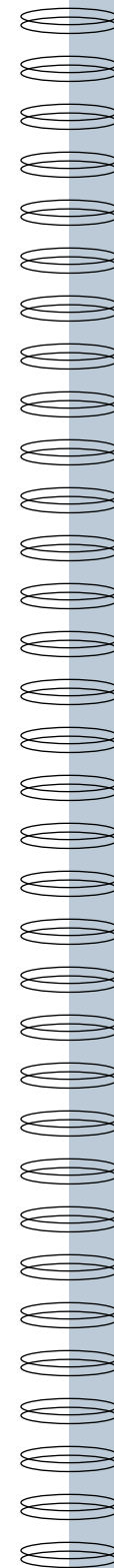
- Abramson S. *The Complete Guide to Cardiac CT*. New York: McGraw Hill Medical; 2012.
- Blanke P, Euringer W, Baumann T, Reinöhl J, Schlensak C, Langer M, Pache G. Combined assessment of aortic root anatomy and aortoiliac vasculature with dual-source CT as a screening tool in patients evaluated for transcatheter aortic valve implantation. *AJR Am J Roentgenol*. 2010 Oct;195(4):872-81.
- Blanke P, Weir-McCall JR, Achenbach S, Delgado V, Hausleiter J, Jilaihawi H, Marwan M, Nørgaard BL, Piazza N, Schoenhagen P, Leipsic JA. Computed Tomography Imaging in the Context of Transcatheter Aortic Valve Implantation (TAVI)/Transcatheter Aortic Valve Replacement (TAVR): An Expert Consensus Document of the Society of Cardiovascular Computed Tomography. *JACC Cardiovasc Imaging*. 2019 Jan;12(1):1-24.
- Barbanti M, Yang T-H, Cabau JR, Tamburino C, Wood DA, Jilaihawi H, Leipsic J. (2013). Anatomical and Procedural Features Associated with Aortic Root Rupture During Balloon-Expandable Transcatheter Aortic Valve Replacement. *Circulation*. 2013; 244-253.
- Blanke P, Schoepf UJ, Leipsic JA. CT in Transcatheter Aortic Valve Replacement. *Radiology*. 2013; 650-669.
- Blanke P, Russe M, Leipsic J, et al. Conformational pulsatile changes of the aortic annulus: impact on prosthesis sizing by computed tomography for transcatheter aortic valve replacement. *JACC Cardiovasc Interv*. September 2012; 5(9):984-94.
- Blanke P, Soon J, Dvir D, Park JK, Naoum C, Kueh SH, Wood DA, Nørgaard BL, Selvakumar K, Ye J, Cheung A, Webb JG, Leipsic J. Computed tomography assessment for transcatheter aortic valve in valve implantation: The vancouver approach to predict anatomical risk for coronary obstruction and other considerations. *J Cardiovasc Comput Tomogr*. 2016 Nov-Dec;10(6): 491-499.
- Blanke P, Naoum C, Dvir D, Bapat V, Ong K, Muller D, Cheung A, Ye J, Min JK, Piazza N, Theriault-Lauzier P, Webb J, Leipsic J. Predicting LVOT Obstruction in Transcatheter Mitral Valve Implantation: Concept of the Neo-LVOT. *JACC Cardiovasc Imaging*. 2017 Apr;10(4):482-485.
- Budoff MJ, Shinbane JS. *Cardiac CT Imaging*. New York: Springer; 2010.
- Frangieh AH, Michel J, Deutsch O, Joner M, Pellegrini C, Rheude T, Bleiziffer S, Kasel AM. Aortic annulus sizing in stenotic bicommissural non-raphe-type bicuspid aortic valves: reconstructing a three-dimensional structure using only two hinge points. *Clin Res Cardiol*. 2019 Jan;108(1):6-15. doi: 10.1007/s00392-018-1295-2. Epub 2018 Jun 14.
- Kasel AM, Cassese S, Bleiziffer S, Amaki M, Hahn R, Kastrati A, Sengupta P. Standardized imaging for aortic annular sizing: implications for transcatheter valve selection. *JACC: Cardiovascular Imaging*. February 2013; 6(2):249-62.
- Kasel AM, Cassese S, Leber AW, von Scheidt W, Kastrati A. Fluoroscopy-guided aortic root imaging for TAVR: “follow the right cusp” rule. *JACC Cardiovasc Imaging*. 2013 Feb;6(2):274-5.
- Leipsic J, Gurvitch R, Troy L, Min J, Wood D, Johnson M, Webb J. Multidetector Computed Tomography in Transcatheter Aortic Valve Implantation. *JACC: Cardiovascular Imaging*. 2011; 416-429.
- Mahesh M, Cody D. AAPM/RSNA Physics Tutorial for Residents: Physics of Cardiac Imaging with Multiple-Row Detector CT. *RadioGraphics*. 2007; 1495-1509. DOI: <http://dx.doi.org/10.1148/rg.275075045>

Ribeiro HB, Rodés-Cabau J, Blanke P, Leipsic J, Kwan Park J, Bapat V, Makkar R, Simonato M, Barbanti M, Schofer J, Bleiziffer S, Latib A, Hildick-Smith D, Presbitero P, Windecker S, Napodano M, Cerillo AG, Abdel-Wahab M, Tchetché D, Fiorina C, Sinning JM, Cohen MG, Guerrero ME, Whisenant B, Nietlispach F, Palma JH, Nombela-Franco L, de Weger A, Kass M, Sandoli de Brito F Jr, Lemos PA, Kornowski R, Webb J, Dvir D. Incidence, predictors, and clinical outcomes of coronary obstruction following transcatheter aortic valve replacement for degenerative bioprosthetic surgical valves: insights from the VIVID registry. *Eur Heart J*. 2018 Feb 21;39(8):687-695

Rist C, Johnson TR, Müller-Starck J, Arnoldi E, Saam T, Becker A, Leber AW, Wintersperger BJ, Becker CR, Reiser MF, Nikolaou K. Noninvasive coronary angiography using dual-source computed tomography in patients with atrial fibrillation. *Invest Radiol*. 2009 Mar;44(3):159-67. doi: 10.1097/RLI.0b013e3181948b05.

Russo M, Tartara P. Trans-Aortic Transcatheter Aortic Valve Replacement with Edwards Sapien-Ascendra 3. 2014, April 10; Retrieved July 1, 2014, from CTSNet: www.ctsnet.org

Schultz CJ, Schoenhagen P, Halliburton SS. *Cardiac CT Made Easy: An Introduction to Cardiovascular Multidetector Computed Tomography*, Second Edition. CRC Press; 2014.



Edwards

This reference book is provided as an educational resource to medical personnel by Edwards Lifesciences (the "Author"). The information in this reference book has been compiled from then-currently available literature. Although every effort has been made to faithfully report the information and keep it up to date, the Author cannot be held responsible for the completeness or accuracy. This reference book is not intended to be and should not be construed as medical advice. For any use, the product information guides, inserts, and operation manuals of the drugs and devices should be consulted. Edwards Lifesciences, and their respective affiliates disclaim any liability arising directly or indirectly from the use of drugs, devices, techniques, or procedures described in this reference book.

WARNING: Any reference to X-ray exposure, intravenous contrast dosage, and other medication is intended as a reference guideline only. The guidelines in this document do not substitute for the judgment of a health care provider. Each scan requires medical judgment by the health care provider about exposing the patient to ionizing radiation. Use the As Low As Reasonably Achievable (ALARA) radiation dose principle to balance factors such as the patient's condition, size, and age; region to be imaged; and diagnostic task.

NOTE: Algorithms/protocols included in this reference book are for educational reference only. The authors do not endorse or support any one specific algorithm/protocol. It is up to each individual clinician and institution to select the treatment that is most appropriate.

Philipp Blanke, MD is a paid consultant for Edwards Lifesciences

Edwards, Edwards Lifesciences and the stylized E logo are trademarks of Edwards Lifesciences Corporation.

© 2021 Edwards Lifesciences Corporation. All rights reserved. DOC-0181400 Rev A

Edwards Lifesciences • One Edwards Way, Irvine CA 92614 USA • edwards.com



Edwards